A New Statistical Technique to Enhance MCGINAR(1) Process Estimates under Symmetric and Asymmetric Data: Fuzzy Time Series Markov Chain and Its Characteristics

Mohammed H. El-Menshawy [1], Abd El-Moneim A. M. Teamah [2], Mohamed S. Eliwa [3,4], Laila A. Al-Essa [5], Mahmoud El-Morshedy [6,7,*] and Rashad M. EL-Sagheer [1,8]

1   Department of Mathematics, Faculty of Science, Al-Azhar University, Nasr City, Cairo 11884, Egypt
2   Department of Mathematics, Faculty of Science, Tanta University, Tanta 31527, Egypt
3   Department of Statistics and Operation Research, College of Science, Qassim University, Buraydah 51482, Saudi Arabia
4   Department of Mathematics, Faculty of Science, Mansoura University, Mansoura 35516, Egypt
5   Department of Mathematical Sciences, College of Science, Princess Nourah bint Abdulrahman University, P.O. Box 84428, Riyadh 11671, Saudi Arabia
6   Department of Mathematics, College of Science and Humanities in Al-Kharj, Prince Sattam bin Abdulaziz University, Al-Kharj 11942, Saudi Arabia
7   Department of Statistics and Computer Science, Faculty of Science, Mansoura University, Mansoura 35516, Egypt
8   High Institute of Computer and Management Information System, First Statement, New Cairo, Cairo 11865, Egypt
*   Correspondence: m.elmorshedy@psau.edu.sa

Abstract: Several models for time series with integer values have been published as a result of the substantial demand for the description of process stability having discrete marginal distributions. One of these models is the mixed count geometric integer autoregressive of order one (MCGINAR(1)), which is based on two thinning operators. This study examines how the estimates of the spectral density functions of the MCGINAR(1) model are affected by fuzzy time series Markov chain (FTSMC). Regarding this study's context, the higher-order moments, central moments and spectral density functions of MCGINAR(1) are computed. The anticipated realizations of the generated realizations for this model are obtained based on FTSMC. In the case of generated and anticipated realizations, several lag windows are used to smooth the spectral density estimators. The generated realization estimates are compared with the anticipated realization estimates using the MSE to ascertain the FTSMC's role in improving the estimation process.

Keywords: FTSMC; time series; spectrum; bispectrum; normalized bispectrum; one- and two-dimensional lag window; fuzzy inference; computer simulation

1. Introduction

Fuzzy time series is an artificial intelligence concept that can be used to perform prediction techniques. Fuzzy time series is based on fuzzy set theory and fuzzy logical relationships. Fuzzy time series can handle data that are configured into linguistic values, such as high, low, median, etc. Fuzzy time series can deal with uncertainty and ambiguity in the data. Fuzzy time series can be used in many applications, such as forecasting stock market indices, recording data, etc. (see [1]).

Fuzzy time series Markov chain for asymmetric and symmetric data is a method of forecasting time series data that have different patterns or behaviors in different directions, such as upward or downward trends. Fuzzy time series Markov chain can handle asymmetric and symmetric data by using different fuzzy sets and Markov chains for each direction of the data. This can improve the accuracy and flexibility of the forecasting model.

Fuzzy time series Markov chain for asymmetric and symmetric data can be used for various applications, such as forecasting air pollution or natural gas prices (see [2–5]).

The modeling of integer-valued time series has received great attention recently; counting series in particular have been the subject of several statistical research works. Thus, there have been numerous significant attempts in this field throughout history. The integer autoregressive (INAR) model works best in modeling counting values. Throughout the past few years, researchers have worked to improve the INAR's ability to accurately simulate observed data. As a result, they have altered some INAR models. A few of them have altered the marginal distribution, while others have changed the models' rankings and yet others have altered the thinning operators. The INAR models were modified with regard to their marginal distribution by [6–9]. The models were modified with regard to their order by [10,11]. INAR models were modified with regard to their thinning operators by [12–18]. Refs. [19–21] presented INAR(1) processes with a random coefficient. A new stationary INAR(1) process with geometric marginals was presented based on the generalized binomial thinning operator in [22]. For several INAR(1) models, ref. [23] studied some statistical measures and used these measurements to support the linearity of the models. Ref. [24] presented an INAR(1) model based on two thinning operators: the first was binomial and the second was a generalized binomial thinning operator, and it was symbolized by MCGINAR(1). Ref. [25] researched the fuzzy time series strategy for the improvement of a periodogram while preserving its statistical features. Ref. [26] studied some statistical measures and spectral density functions for a zero truncated Poisson integer autoregressive (ZTPINAR(1)) model. Ref. [27] used the fuzzy principle on the smoothing estimates for the dependent count geometric integer autoregressive (DCGINAR(1)) process.

This paper aims to introduce the FTSMC approach for the improvement of the estimates of density functions for integer time series. This approach is used with the MCGINAR(1) model. Prior to applying this approach, some statistical measures, namely higher-order statistics for the MCGINAR(1) model, are studied. These measures are moments, cumulants, spectral density functions, and the estimates for these functions. For the MCGINAR(1) series, we apply FTSMC in [28] and forecast realizations for this series. Two scenarios are used to estimate the density functions: produced realizations from the MCGINAR(1) model and anticipated realizations based on the FTSMC technique. The role that FTSMC plays in the smoothing of these estimates is investigated by contrasting the two scenarios using results and figures.

2. Fuzzy Time Series Markov Chain: A New Statistical Approach and Its Methodology

Fuzzy time series and conventional time series vary primarily in that the former's values are fuzzy sets and the latter's values are actual numbers. We describe a method [28] in this section to transform regular time series into fuzzy time series and forecasting observations for the final series. The nine steps of this strategy, which uses FTSMC to improve the forecasting accuracy, are as follows.

1. Determine the universe set $\mathbb{H} = [Y_{min}, Y_{max}]$, where Y_{min} and Y_{max} are, respectively, the smallest and largest values of the generated realizations from the MCGINAR(1) model, respectively.
2. The universe set $\mathbb{H}$ is partitioned into a number of identically sized intervals. The Sturges formula, $d = 3.322\log(N) + 1$, can be used to determine how many intervals are required, and, to define the length of each interval l, formula $l = (Y_{max} - Y_{min})/(d)$ is used.
3. Generate fuzzy sets on $\mathbb{H}$ and fuzzify the realizations produced by the MCGINAR(1) model.
4. Based on the generated realizations from the MCGINAR(1) model, determine the fuzzy logic relationship.
5. Establish fuzzy logic relation groups by creating groups from the fuzzy logic relations.
6. As described in the previous stage, determine the transition probability matrix p based on the fuzzy logic relation group. The dimension of the Markov transition probability matrix is p by p, where p is the total number of fuzzy sets. The state

transition probability is expressed as $p_{ij} = \frac{I_{ij}}{I_i}$, where p_{ij} = transition probability from state A_i to A_j, I_{ij} = number of transitions from state A_i to A_j, and I_i = number of data included in state A_i.

7. Calculate the prediction value for the fuzzy observation.

Rule 1: When data from the $(t-1)$ interval are included in A_i and there are fuzzy sets, such as $A_i \rightarrow \phi$, which do not have fuzzy logic relations, the prediction value F_t is $m_{i(t-1)}$, which is the median of the u_i interval on the fuzzy logic relation group that was developed in the $(t-1)$ data.

Rule 2: If fuzzy logic relation group A_i has a one-to-one relation (for example, $A_i \rightarrow A_p$, where $p_{ip} = 1$ and $p_{ij} = 0, j \neq p$), where the collected data are Y_{t-1} in $(t-1)$ time included in state A_i, then the prediction value of F_t is $m_{p(t-1)}$, where $m_{p(t-1)}$ is the median of u_p in the fuzzy logic relation group that formed on the $(t-1)$ data.

Rule 3: If fuzzy logic relation group A_i has a one-to-many relation (for example, $A_j \rightarrow A_1, A_2, \ldots A_q, J = 1, 2, \ldots q$), where the collected data are Y_{t-1} in $(t-1)$ time included in state A_i, then the prediction value of F_t is $F_t = m_{1(t-1)}P_{j1} + m_{2(t-1)}P_{j2} + \ldots m_{(j-1)(t-1)}P_{j(j-1)} + Y_{t-1}P_{jj} + m_{(j+1)(t-1)}P_{j(j+1)} + \ldots m_{q(t-1)}P_{jq}$.

8. Apply the result for the payment of the forecasting value.

Rule 1: The adjustment value of D_t is defined as $D_{t1} = \frac{l}{2}$, where l is the length of the interval if state A_i is related to A_i, starting from state A_i at time $t-1$ as $F_{t-1} = A_i$, and making an ascending transition to state A_i at time t, where $i < j$.

Rule 2: The adjustment value of D_t is defined as $D_{t1} = \frac{-l}{2}$, where l if state A_i is related to A_i, starting from state A_i at time $t-1$ as $F_{t-1} = A_i$, and making a downward transition to state A_i at time t, where $i > j$.

Rule 3: The trend adjustment value of D_t is defined as $D_{t1} = (\frac{-l}{2})s$, with s being the number of leaps ahead if the transition starts from state Ai at time $t-1$ as $F_{t-1} = A_i$, and jumps forward to state A_{i+s} at time t where $(1 \leq s \leq p - i)$.

Rule 4: The trend adjustment value of D_t is defined as $D_{t1} = (\frac{-l}{2})v$, with v being a lot of backward jumps if the transition starts from state A_i at time $t-1$ as $F_{t-1} = A_i$, and jumps back to state A_{i-v} at time t where $(1 \leq v \leq i)$.

9. Adjust the predictive value of forecasting to ascertain the outcomes. If the fuzzy logic relation group A_i is one-to-many and state A_{i+1} can be retrieved from A_i, where A_i state is related to A_i, the forecasting result is $F'_t = F_t + D_{t1}$.

For more details about this method, see [28–30]. Thus, the anticipated realizations are the output of this method, which was applied to the generated realizations from MCGINAR(1).

3. The MCGINAR(1) Process

There are some real-world events that are neither entirely autonomous nor entirely reliant. For illustration, consider a data set that is received from a police telephone service and shows the monthly total of calls reporting guns fired. We cannot declare with certainty that the counting series, which would model such data, should contain completely dependent or completely independent variables because the calls may be tied to an organized crime or to crimes unrelated to one another. Therefore, some scientists went a step further and developed a new model called the MCGINAR(1) model, which is based on a combination of dependent and independent counting variables. The MCGINAR(1) model was firstly defined by [24] and takes the following formula:

$$Y_t = \begin{cases} \gamma \circ Y_{t-1} + \varepsilon_t & \text{W.P} \quad q, \\ \gamma \circ_\vartheta Y_{t-1} + \varepsilon_t & \text{W.P} \quad 1-q, \end{cases} \quad \gamma, \vartheta, q \in [0,1], t \geq 1. \tag{1}$$

For all the characteristics of the binomial thinning operator $\gamma\circ$ and the generalized binomial thinning operator $\gamma\circ_\vartheta$, see [22,24,31]. $\{Y_t\}$ has a geometric $\left(\frac{v}{1+v}\right)$ marginal distribution with mean $v > 0$.

The probability generating functions of Y_t and ε_t are, respectively, given by (see [24])

$$\phi_Y(s) = \frac{1}{1 + v - vs},$$

$$\phi_\varepsilon(s) = \frac{(1 + c_1(1-\vartheta)v - \gamma(1-\vartheta)vs)(1+\gamma v - \gamma vs)(1 + \gamma v + \vartheta v - \gamma\vartheta v - (\gamma + \vartheta - \gamma\vartheta)vs)}{(1 + v - vs)(1 + c_1 v - c_1 vs)(1 + c_2 v - c_2 vs)},$$

where c_1 and c_2 are solutions of $z^2 - (2\gamma + \vartheta - 2\gamma\vartheta)z + \gamma(\gamma + \vartheta - 2\gamma\vartheta - \vartheta^2 p + \gamma\vartheta^2 p) = 0$. The mean and variance of Y_t and ε_t are, respectively, given by

$$\mu_Y = v, \quad \sigma_Y^2 = v^2 + v,$$

$$\mu_\varepsilon = v - \gamma v, \quad \sigma_\varepsilon^2 = (v - \gamma v)(1 + (1 + \gamma - 2\gamma(1-q)\vartheta^2)v).$$

The second and third moments of ε_t are, respectively, calculated as

$$E(\varepsilon^2) = (1 - \gamma)v(1 + 2(1 - \gamma(1-q)\vartheta^2)v), \tag{2}$$

$$\begin{aligned} E(\varepsilon^3) =&(1-\gamma)v(6v + 6v^2 - 6\gamma\vartheta^2 v - 6\gamma\vartheta^2 v^2 - 6\gamma\vartheta^3 v^2 - 6\gamma^2\vartheta^2 v^2 + 12\gamma^2\vartheta^3 v^2 + 6\gamma^2 q\vartheta^2 v^2 \\ &- 12\gamma^2 q\vartheta^3 v^2 + 6\gamma q\vartheta^2 v + 6\gamma q\vartheta^2 v^2 + 6\gamma q\vartheta^3 v^2 + 1). \end{aligned} \tag{3}$$

For more information about the MCGINAR(1) model, see [24].

4. Higher-Order Joint Moments, Central Moments, and Spectral Density Functions

In this section, the moments, cumulants, spectrum, and bispectrum of MCGINAR(1) are given. These statistical measures have a role in describing the stochastic process. For the importance of these statistical measures, the following theorems were concluded.

Theorem 1. *Let $\{Y_t\}$, satisfying (1). Then,*

1. *The second-order joint moment is calculated as*

$$\mu_{(s)} = \gamma^s[\mu_{(0)} - v^2] + v^2 = \gamma^s v(1 + v) + v^2, s \geq 0 \text{ and } v_{(0)} = v(1 + 2v).$$

2. *The second-order joint central moment (cumulant) is*

$$C_2(s) = \gamma^s C_2(0) = \gamma^s v(1 + v), s \geq 0.$$

3. *The third-order joint moments are*

$$\mu_{(0,0)} = v(1 + 6v + 6v^2),$$

$$\mu_{(0,s)} = \gamma^s[\mu_{(0,0)} - v\mu_{(0)}] + v\mu_{(0)} = v^2(1 + 2v) + \gamma^s v(1 + 5v + 4v^2), s \geq 0,$$

$$\mu_{(s,s)} = g^s\mu_{(0,0)} + hC_2(0)\frac{\gamma^s - g^s}{\gamma - g} + [hv^2 + vE(\varepsilon^2)]\frac{1 - g^s}{1 - g},$$

where

$$g = \gamma(\gamma + (1-\gamma)\vartheta^2) - q(\gamma - \gamma^2)\vartheta^2, \tag{4}$$

and

$$h = 2\gamma\mu_\varepsilon + (\gamma - \gamma^2)(1 - \vartheta^2) + p\vartheta^2(\gamma - \gamma^2). \tag{5}$$

4. *The third-order joint central moments (cumulants) are*

$$C_3(0,0) = v(1 + 3v + 2v^2),$$

$$C_3(0,s) = \gamma^s C_3(0,0) = \gamma^s v(1 + 3v + 2v^2), s \geq 0,$$

$$C_3(s,s) = g^s C_3(0,0) + [2gv - 2\gamma v + h]C_2(0)\left[\frac{\gamma^s - g^s}{\gamma - g}\right],$$

where g and h are, respectively, given by (4) and (5).

$$C_3(s,\tau) = \gamma^{\tau-s} C_3(s,s).$$

Proof. $\mu_{(0)} = E(Y_t^2)$ is computed as

$$
\begin{aligned}
E(Y_t^2) &= qE(\gamma \circ Y_{t-1} + \varepsilon_t)^2 + (1-q)E(\gamma \circ_\vartheta Y_{t-1} + \varepsilon_t)^2 \\
&= q[E(\gamma \circ_\vartheta Y_{t-1})^2 + E(\varepsilon_t^2) + 2\gamma E(Y_{t-1})E(\varepsilon_t)] + (1-q)[E(\gamma \circ_\vartheta Y_{t-1}^2) + E(\varepsilon_t^2) + 2\gamma\mu_\varepsilon\mu_Y] \\
&= q[\gamma^2 E(Y_{t-1}^2) + \gamma(1-\gamma)E(Y_{t-1}) + E(\varepsilon^2) + 2\gamma\mu_Y\mu_\varepsilon] + (1-q)[\gamma(\gamma + \vartheta^2(1-\gamma))E(Y_{t-1}^2) \\
&\quad + \gamma(1-\gamma)(1-\vartheta^2)E(Y_{t-1}) + E(\varepsilon^2) + 2\gamma\mu_Y\mu_\varepsilon] \\
&= (q\gamma^2 + (1-q)(\gamma^2 + \gamma(1-\gamma)\vartheta^2))E(Y_{t-1}^2) + q\gamma(1-\gamma)E(Y_{t-1}) + (1-q)\gamma(1-\gamma)(1-\vartheta^2)E(Y_{t-1}) \\
&\quad + E(\varepsilon^2)
\end{aligned}
$$

$$E(Y_t^2) = (\gamma^2 + (1-q)\gamma(1-\gamma)\vartheta^2)E(Y_{t-1}^2) + E(Y_{t-1})\gamma(1-\gamma)(q + (1-q)(1-\vartheta^2)) + 2\gamma\mu_Y\mu_\varepsilon + E(\varepsilon^2),$$

and, therefore,

$$E(Y_t^2)(1 - (\gamma^2 + \gamma(1-\gamma)\vartheta^2(1-q)) = \mu_Y\gamma(1-\gamma)(1 - \vartheta^2(1-q)) + \sigma_\varepsilon^2 + \mu_\varepsilon^2 + 2\gamma\mu_Y\mu_\varepsilon$$

then,

$$E(Y_t^2) = \frac{v(1+2v)(1 - \gamma^2 - \gamma(1 - \gamma\vartheta^2(1-q)))}{(1 - \gamma^2 - \gamma(1 - \gamma\vartheta^2(1-q)))} = v(1 + 2v),$$

then,

$$C_2(0) = \mu_{(0)} - \mu_Y^2 = v(1 + 2v) - v^2 = v(1 + v).$$

$\mu_{(s)}$ is obtained by

$$
\begin{aligned}
\mu_{(s)} &= E(Y_t Y_{t+s}) = (1-q)E(Y_t(\gamma_{t+s} \circ_\vartheta Y_{t+s-1} + \varepsilon_{t+s})) + qE(Y_t(\gamma_{t+s} \circ Y_{t+s-1} + \varepsilon_{t+s})) \\
&= (1-q)[E(Y_t(\gamma \circ_\vartheta Y_{t+s-1})) + E(Y_t\varepsilon_{t+s})] + q[E(Y_t(\gamma \circ Y_{t+s-1})) + E(Y_t\varepsilon_{t+s})] \\
&= (1-q)[\gamma\mu_{(s-1)} + \mu_Y\mu_\varepsilon] + q[\gamma\mu_{(s-1)} + \mu_Y\mu_\varepsilon] = \gamma\mu_{(s-1)} + \mu_Y\mu_\varepsilon,
\end{aligned}
$$

and by solving this equation using the Maple program or by iteration and simplification,

$$\mu_{(s)} = \gamma^s \mu_{(0)} + \frac{1 - \gamma^s}{1 - \gamma}\mu_Y\mu_\varepsilon = \gamma^s v(1 + v) + v^2,$$

then,

$$C_2(s) = \mu_{(s)} - \mu_Y^2 = \gamma^s v(1 + v) + v^2 - v^2 = \gamma^s C_2(0).$$

$\mu_{(0,s)}$ is calculated as

$$
\begin{aligned}
\mu_{(0,s)} &= E(Y_t Y_t Y_{t+s}) = (1-q)E[Y_t Y_t(\gamma_{t+s} \circ_\vartheta Y_{t+s-1} + \varepsilon_{t+s})] + qE[Y_t Y_t(\gamma_{t+s} \circ Y_{t+s-1} + \varepsilon_{t+s})] \\
&= (1-q)[E(Y_t Y_t(\gamma \circ_\vartheta Y_{t+s-1})) + E(Y_t Y_t\varepsilon_{t+s})] + q[E(Y_t Y_t(\gamma \circ Y_{t+s-1})) + E(Y_t Y_t\varepsilon_{t+s})] \\
&= (1-q)[\gamma E(Y_t Y_t Y_{t+s-1}) + E(Y_t^2)\mu_\varepsilon] + q[\gamma E(Y_t Y_t Y_{t+s-1}) + E(Y_t^2)\mu_\varepsilon] \\
&= (1-q)[\gamma\mu_{(0,s-1)} + \mu_{(0)}\mu_\varepsilon] + q[\gamma\mu_{(0,s-1)} + \mu_{(0)}\mu_\varepsilon] = \gamma\mu_{(0,s-1)} + \mu_{(0)}\mu_\varepsilon,
\end{aligned}
$$

by iteration and simplification,

$$\mu_{(0,s)} = \gamma^s \mu_{(0,0)} + (1 - \gamma^s) v \mu_{(0)} = v^2(1 + 2v) + \gamma^s v(1 + 5v + 4v^2),$$

then,

$$
\begin{aligned}
C_3(0,s) &= E[(Y_t - v)^2(Y_{t+s} - v)] = \mu_{(0,s)} - 2\mu_Y \mu_{(s)} - \mu_Y \mu_{(0)} + 2\mu_Y^3 = \gamma\mu_{(0,s-1)} + \mu_{(0)}\mu_\varepsilon \\
&\quad - 2v(\gamma\mu_{(s-1)} + v\mu_\varepsilon) - v\mu_{(0)} + 2v^3 = \gamma\mu_{(0,s-1)} + (1 - \gamma)v\mu_{(0)} - 2v(\gamma\mu_{(s-1)} + v^2(1 - \gamma)) \\
&\quad - v\mu_{(0)} + 2v^3 = \gamma[\mu_{(0,s-1)} - v\{2\mu_{(s-1)} + \mu_{(0)}\} + 2v^3] = \gamma C_3(0, s-1) = v^2(1 + 2v) + \\
&\quad \gamma^s v(1 + 5v + 4v^2) - 2v(\gamma^s(v^2 + v) + v^2) - v^2(2v + 1) + 2v^3 = \gamma^s v(1 + 3v + 2v^2).
\end{aligned}
$$

In the same manner, the proof can be completed. $\square$

Theorem 2. *The spectral density function is computed as*

$$f_{YY}(w) = \frac{v(1 + v)(1 - \gamma^2)}{2\pi(1 + \gamma^2 - 2\gamma \cos w)}, \quad -\pi \leq w \leq \pi. \tag{6}$$

Proof.

$$
\begin{aligned}
f_{YY}(w) &= \frac{1}{2\pi} \sum_{s=-\infty}^{\infty} C_2(s) \exp(-iws) = \frac{1}{2\pi}\left[C_2(0) + \sum_{s=1}^{\infty} C_2(s)\exp(-iws) + \sum_{s=-\infty}^{-1} C_2(s)\exp(-iws)\right] \\
&= \frac{1}{2\pi}\left[C_2(0) + \sum_{s=1}^{\infty} \gamma^s C_2(0)\exp(-iws) + \sum_{s=1}^{\infty} \gamma^s C_2(0)\exp(iws)\right] \\
&= \frac{C_2(0)}{2\pi}\left[1 + \frac{\gamma\exp(-iw)}{1 - \gamma\exp(-iw)} + \frac{\gamma\exp(iw)}{1 - \gamma\exp(iw)}\right] = \frac{C_2(0)}{2\pi}\left[\frac{(1 - \gamma^2)}{(1 - \gamma\exp(-iw))(1 - \gamma\exp(iw))}\right].
\end{aligned}
$$

$\square$

Theorem 3. *The bispectral density function is calculated as*

$$
\begin{aligned}
f_{YYY}(w_1, w_2) &= \frac{1}{4\pi^2}\Big[C_3(0,0)\{1 + I_1(-w_1) + I_1(-w_2) + I_1(w_1 + w_2)\} \\
&\quad + (C_3(0,0) - \frac{[2g\mu_Y - 2\gamma\mu_Y + h]C_2(0)}{\gamma - g})(I_2(w_1) + I_2(w_2) + I_2(-w_1 - w_2)) \\
&\quad + (\frac{[2g\mu_Y - 2\gamma\mu_Y + h]C_2(0)}{\gamma - g})\{I_1(w_1) + I_1(w_2) + I_1(-w_1 - w_2)\} \\
&\quad + (C_3(0,0) - \frac{[2g\mu_Y - 2\gamma\mu_Y + h]C_2(0)}{\gamma - g})\{I_2(-w_1 - w_2)I_1(-w_2) \\
&\quad + I_2(-w_1 - w_2)I_1(-w_1) + I_2(w_1)I_1(-w_2) + I_2(w_2)I_1(-w_1) + I_2(w_1)I_1(w_1 + w_2) \\
&\quad + I_2(w_2)I_1(w_1 + w_2)\} + (\frac{[2g\mu_Y - 2\gamma\mu_Y + h]C_2(0)}{\gamma - g})\{I_1(-w_1 - w_2)I_1(-w_2) \\
&\quad + I_1(-w_1 - w_2)I_1(-w_1) + I_1(w_1)I_1(-w_2) + I_1(w_2)I_1(-w_1) + I_1(w_1)I_1(w_1 + w_2) \\
&\quad + I_1(w_2)I_1(w_1 + w_2)\}\Big],
\end{aligned}
\tag{7}
$$

where $I_1(w_k) = \frac{\gamma\exp(iw_k)}{1 - \gamma\exp(iw_k)}$ *and* $I_2(w_k) = \frac{A\exp(iw_k)}{1 - A\exp(iw_k)}, k = 1, 2,$ *and* $-\pi \leq w_1, w_2 \leq \pi$. *A and B are, respectively, given by (4) and (5).*

Proof. The proof of this theorem is too long to be included here and it is similar to the proof of Theorem 2 in [26]. The normalized bispectral $g_{YYY}(w_1, w_2)$ is calculated as

$$g_{YYY}(w_1, w_2) = \frac{f_{YYY}(w_1, w_2)}{\sqrt{f_{YY}(w_1)f_{YY}(w_2)f_{YY}(w_1 + w_2)}}, \tag{8}$$

where $f_{YYY}(w_1, w_2)$ and $f_{YY}(w_1)$ are defined in (6) and (7). $\square$

Figure 1 illustrates a simulated series of the MCGINAR(1) model at $\gamma = 0.7$, $\vartheta = 0.5$, and $v = 1.9$. Figure 2 illustrates a simulated series of the anticipated MCGINAR(1) realizations based on FTSMC. Figure 3 shows the theoretical spectrum $f_{YY}(w)$, which was calculated by setting $\gamma = 0.7$ and $v = 1.9$ in (6). Figure 4 shows the theoretical bispectral $f_{YYY}(w_1, w_2)$, which was calculated by setting $\gamma = 0.7$, $\vartheta = 0.5$, and $v = 1.9$ in (7), and the results of this function are shown in Table 1. Figure 5 shows the theoretical normalized bispectral $g_{YYY}(w_1, w_2)$, which was calculated by (8), and the results of this function are shown in Table 2.
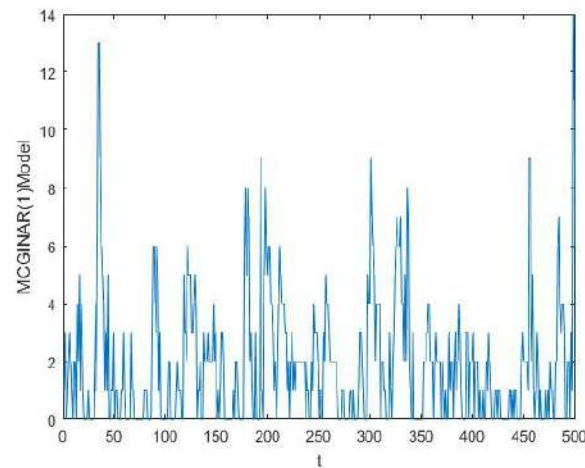
Figure 1. Simulated series of MCGINAR(1) at $\gamma = 0.7$, $\vartheta = 0.5$, and $v = 1.9$.
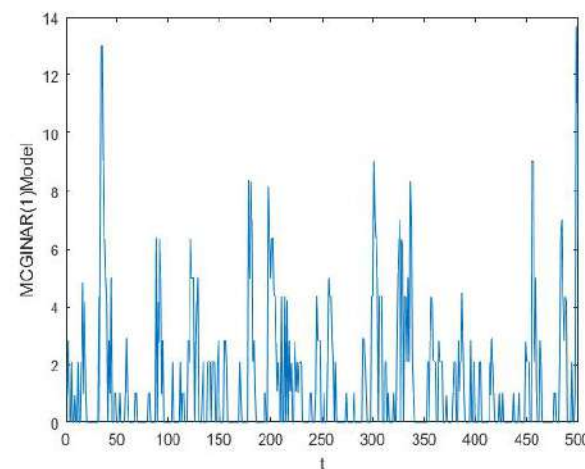
Figure 2. Simulated series of anticipated MGINAR(1) realizations based on FTSMC.
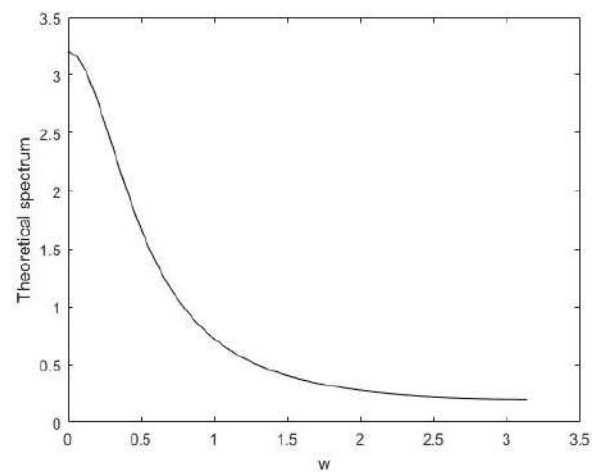
Figure 3. The spectral density of MCGINAR(1) at $\gamma = 0.7$ and $v = 1.9$.

Figure 4. Bispectral density of MCGINAR(1) at $\gamma = 0.7$, $\vartheta = 0.5$, and $v = 1.9$.

Figure 5. Normalized bispectral density of MCGINAR(1) at $\gamma = 0.7$, $\vartheta = 0.5$, and $v = 1.9$.

Table 1. Numerical values of theoretical bispectrum modulus of MCGINAR(1) with $\gamma = 0.7$, $\vartheta = 0.5$, and $v = 1.9$.

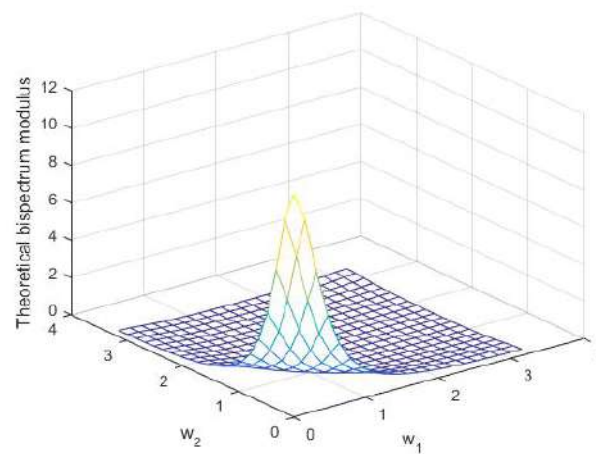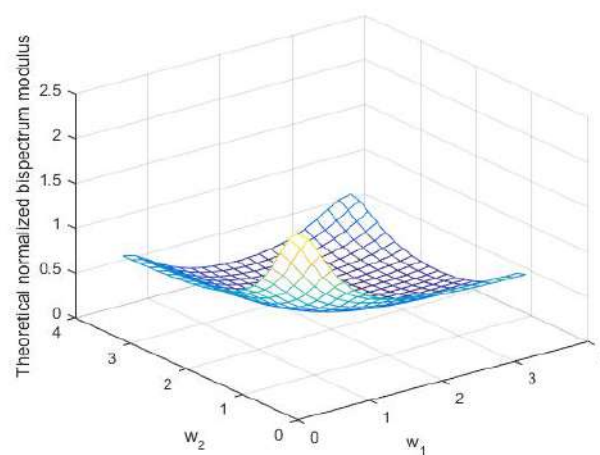| w_2	0.00 π	0.05 π	0.10 π	0.15 π	0.20 π	0.25 π	0.30 π	0.35 π	0.40 π	0.45 π	0.50 π	0.55 π	0.60 π	0.65 π	0.70 π	0.75 π	0.80 π	0.85 π	0.90 π	0.95 π	π
w_1																					
0.00 π	11.937	10.436	7.4683	4.9546	3.3081	2.2974	1.6713	1.2702	1.0033	0.8192	0.6882	0.5927	0.5216	0.4681	0.4275	0.3967	0.3737	0.3570	0.3457	0.3391	0.3370
0.05 π	10.436	8.2535	5.6847	3.7802	2.5711	1.8253	1.3556	1.0492	0.8417	0.6966	0.5921	0.5152	0.4576	0.4141	0.3811	0.3562	0.3379	0.3249	0.3167	0.3126	0.3126
0.10 π	7.4683	5.6847	3.9216	2.6524	1.8404	1.3310	1.0046	0.7884	0.6401	0.5352	0.4591	0.4028	0.3605	0.3286	0.3044	0.2864	0.2734	0.2645	0.2594	0.2577	0.2594
0.15 π	4.9546	3.7802	2.6524	1.8287	1.2912	0.9477	0.7243	0.5744	0.4707	0.3969	0.3430	0.3030	0.2730	0.2504	0.2334	0.2209	0.2121	0.2065	0.2038	0.2038	0.2065
0.20 π	3.3081	2.5711	1.8404	1.2912	0.9248	0.6868	0.5301	0.4240	0.3501	0.2972	0.2585	0.2298	0.2083	0.1921	0.1801	0.1715	0.1657	0.1623	0.1612	0.1623	0.1657
0.25 π	2.2974	1.8253	1.3310	0.9477	0.6868	0.5150	0.4007	0.3229	0.2683	0.2292	0.2005	0.1792	0.1634	0.1515	0.1429	0.1369	0.1330	0.1312	0.1312	0.1330	0.1369
0.30 π	1.6713	1.3556	1.0046	0.7243	0.5301	0.4007	0.3140	0.2546	0.2128	0.1828	0.1608	0.1446	0.1325	0.1236	0.1172	0.1130	0.1105	0.1097	0.1105	0.1130	0.1172
0.35 π	1.2702	1.0492	0.7884	0.5744	0.4240	0.3229	0.2546	0.2076	0.1745	0.1507	0.1333	0.1205	0.1110	0.1042	0.0994	0.0964	0.0950	0.0950	0.0964	0.0994	0.1042
0.40 π	1.0033	0.8417	0.6401	0.4707	0.3501	0.2683	0.2128	0.1745	0.1475	0.1281	0.1139	0.1035	0.0959	0.0906	0.0870	0.0849	0.0842	0.0849	0.0870	0.0906	0.0959
0.45 π	0.8192	0.6966	0.5352	0.3969	0.2972	0.2292	0.1828	0.1507	0.1281	0.1118	0.1000	0.0914	0.0852	0.0809	0.0783	0.0770	0.0770	0.0783	0.0809	0.0852	0.0914
0.50 π	0.6882	0.5921	0.4591	0.3430	0.2585	0.2005	0.1608	0.1333	0.1139	0.1000	0.0899	0.0827	0.0776	0.0742	0.0723	0.0716	0.0723	0.0742	0.0776	0.0827	0.0899
0.55 π	0.5927	0.5152	0.4028	0.3030	0.2298	0.1792	0.1446	0.1205	0.1035	0.0914	0.0827	0.0765	0.0723	0.0696	0.0684	0.0684	0.0696	0.0723	0.0765	0.0827	0.0914
0.60 π	0.5216	0.4576	0.3605	0.2730	0.2083	0.1634	0.1325	0.1110	0.0959	0.0852	0.0776	0.0723	0.0688	0.0668	0.0662	0.0668	0.0688	0.0723	0.0776	0.0852	0.0959
0.65 π	0.4681	0.4141	0.3286	0.2504	0.1921	0.1515	0.1236	0.1042	0.0906	0.0809	0.0742	0.0696	0.0668	0.0654	0.0654	0.0668	0.0696	0.0742	0.0809	0.0906	0.1042
0.70 π	0.4275	0.3811	0.3044	0.2334	0.1801	0.1429	0.1172	0.0994	0.0870	0.0783	0.0723	0.0684	0.0662	0.0654	0.0662	0.0684	0.0723	0.0783	0.0870	0.0994	0.1172
0.75 π	0.3967	0.3562	0.2864	0.2209	0.1715	0.1369	0.1130	0.0964	0.0849	0.0770	0.0716	0.0684	0.0668	0.0668	0.0684	0.0716	0.0770	0.0849	0.0964	0.1130	0.1369
0.80 π	0.3737	0.3379	0.2734	0.2121	0.1657	0.1330	0.1105	0.0950	0.0842	0.0770	0.0723	0.0696	0.0688	0.0696	0.0723	0.0770	0.0842	0.0950	0.1105	0.1330	0.1657
0.85 π	0.3570	0.3249	0.2645	0.2065	0.1623	0.1312	0.1097	0.0950	0.0849	0.0783	0.0742	0.0723	0.0723	0.0742	0.0783	0.0849	0.0950	0.1097	0.1312	0.1623	0.2065
0.90 π	0.3457	0.3167	0.2594	0.2038	0.1612	0.1312	0.1105	0.0964	0.0870	0.0809	0.0776	0.0765	0.0776	0.0809	0.0870	0.0964	0.1105	0.1312	0.1612	0.2038	0.2594
0.95 π	0.3391	0.3126	0.2577	0.2038	0.1623	0.1330	0.1130	0.0994	0.0906	0.0852	0.0827	0.0827	0.0852	0.0906	0.0994	0.1130	0.1330	0.1623	0.2038	0.2577	0.3126
π	0.3370	0.3126	0.2594	0.2065	0.1657	0.1369	0.1172	0.1042	0.0959	0.0914	0.0899	0.0914	0.0959	0.1042	0.1172	0.1369	0.1657	0.2065	0.2594	0.3126	0.3370

Table 2. Numerical values of theoretical normalized bispectrum modulus of MCGINAR(1) with $\gamma = 0.7$, $\vartheta = 0.5$, and $v = 1.9$.

w_2	0.00 π	0.05 π	0.10 π	0.15 π	0.20 π	0.25 π	0.30 π	0.35 π	0.40 π	0.45 π	0.50 π	0.55 π	0.60 π	0.65 π	0.70 π	0.75 π	0.80 π	0.85 π	0.90 π	0.95 π	π
w_1																					
0.00 π	2.0770	1.9834	1.7764	1.5668	1.4001	1.2778	1.1898	1.1261	1.0792	1.0443	1.0178	0.9975	0.9818	0.9696	0.9601	0.9527	0.9471	0.9430	0.9402	0.9386	0.9380
0.05 π	1.9834	1.8341	1.6295	1.4453	1.3038	1.2004	1.1255	1.0708	1.0302	0.9997	0.9764	0.9584	0.9444	0.9336	0.9251	0.9186	0.9138	0.9103	0.9081	0.9070	0.9070
0.10 π	1.7764	1.6295	1.4548	1.3006	1.1812	1.0928	1.0279	0.9799	0.9439	0.9166	0.8956	0.8794	0.8668	0.8569	0.8493	0.8435	0.8393	0.8364	0.8347	0.8341	0.8347
0.15 π	1.5668	1.4453	1.3006	1.1698	1.0662	0.9882	0.9302	0.8867	0.8539	0.8288	0.8094	0.7943	0.7826	0.7734	0.7665	0.7612	0.7575	0.7551	0.7539	0.7539	0.7551
0.20 π	1.4001	1.3038	1.1812	1.0662	0.9731	0.9020	0.8483	0.8078	0.7769	0.7532	0.7349	0.7206	0.7095	0.7009	0.6944	0.6896	0.6864	0.6845	0.6839	0.6845	0.6864
0.25 π	1.2778	1.2004	1.0928	0.9882	0.9020	0.8351	0.7843	0.7457	0.7161	0.6933	0.6757	0.6619	0.6513	0.6432	0.6371	0.6328	0.6300	0.6286	0.6286	0.6300	0.6328
0.30 π	1.1898	1.1255	1.0279	0.9302	0.8483	0.7843	0.7353	0.6979	0.6692	0.6471	0.6299	0.6166	0.6064	0.5986	0.5930	0.5891	0.5869	0.5861	0.5869	0.5891	0.5930
0.35 π	1.1261	1.0708	0.9799	0.8867	0.8078	0.7457	0.6979	0.6613	0.6332	0.6116	0.5948	0.5819	0.5721	0.5648	0.5596	0.5562	0.5546	0.5546	0.5562	0.5596	0.5648
0.40 π	1.0792	1.0302	0.9439	0.8539	0.7769	0.7161	0.6692	0.6332	0.6056	0.5844	0.5680	0.5555	0.5460	0.5391	0.5345	0.5318	0.5309	0.5318	0.5345	0.5391	0.5460
0.45 π	1.0443	0.9997	0.9166	0.8288	0.7532	0.6933	0.6471	0.6116	0.5844	0.5635	0.5475	0.5353	0.5264	0.5200	0.5159	0.5140	0.5140	0.5159	0.5200	0.5264	0.5353
0.50 π	1.0178	0.9764	0.8956	0.8094	0.7349	0.6757	0.6299	0.5948	0.5680	0.5475	0.5319	0.5202	0.5117	0.5060	0.5027	0.5016	0.5027	0.5060	0.5117	0.5202	0.5319
0.55 π	0.9975	0.9584	0.8794	0.7943	0.7206	0.6619	0.6166	0.5819	0.5555	0.5353	0.5202	0.5090	0.5012	0.4962	0.4938	0.4938	0.4962	0.5012	0.5090	0.5202	0.5353
0.60 π	0.9818	0.9444	0.8668	0.7826	0.7095	0.6513	0.6064	0.5721	0.5460	0.5264	0.5117	0.5012	0.4941	0.4900	0.4887	0.4900	0.4941	0.5012	0.5117	0.5264	0.5460
0.65 π	0.9696	0.9336	0.8569	0.7734	0.7009	0.6432	0.5986	0.5648	0.5391	0.5200	0.5060	0.4962	0.4900	0.4870	0.4870	0.4900	0.4962	0.5060	0.5200	0.5391	0.5648
0.70 π	0.9601	0.9251	0.8493	0.7665	0.6944	0.6371	0.5930	0.5596	0.5345	0.5159	0.5027	0.4938	0.4887	0.4870	0.4887	0.4938	0.5027	0.5159	0.5345	0.5596	0.5930
0.75 π	0.9527	0.9186	0.8435	0.7612	0.6896	0.6328	0.5891	0.5562	0.5318	0.5140	0.5016	0.4938	0.4900	0.4900	0.4938	0.5016	0.5140	0.5318	0.5562	0.5891	0.6328
0.80 π	0.9471	0.9138	0.8393	0.7575	0.6864	0.6300	0.5869	0.5546	0.5309	0.5140	0.5027	0.4962	0.4941	0.4962	0.5027	0.5140	0.5309	0.5546	0.5869	0.6300	0.6864
0.85 π	0.9430	0.9103	0.8364	0.7551	0.6845	0.6286	0.5861	0.5546	0.5318	0.5159	0.5060	0.5012	0.5012	0.5060	0.5159	0.5318	0.5546	0.5861	0.6286	0.6845	0.7551
0.90 π	0.9402	0.9081	0.8347	0.7539	0.6839	0.6286	0.5869	0.5562	0.5345	0.5200	0.5117	0.5090	0.5117	0.5200	0.5345	0.5562	0.5869	0.6286	0.6839	0.7539	0.8347
0.95 π	0.9386	0.9070	0.8341	0.7539	0.6845	0.6300	0.5891	0.5596	0.5391	0.5264	0.5202	0.5202	0.5264	0.5391	0.5596	0.5891	0.6300	0.6845	0.7539	0.8341	0.9070
π	0.9380	0.9070	0.8347	0.7551	0.6864	0.6328	0.5930	0.5648	0.5460	0.5353	0.5319	0.5353	0.5460	0.5648	0.5930	0.6328	0.6864	0.7551	0.8347	0.9070	0.9380

5. Estimation of Spectral Density Functions

The bispectral density function provides useful information about the non-linearity of the process. For continuous non-Gaussian time series, the modulus of the normalized bispectrum is flat. From Figures 4 and 5, we can conclude that the model is linear; since the values of the theoretical normalized bispectrum lie within (0.4, 2.5), they are flatter (constant—lying very closely to each other) than the values of the non-normalized one that lies within (0, 12).

The smoothed periodogram approach is used to estimate the spectral density functions using the simulated series from the MCGINAR(1) model with $\{Y_t, t = 1, 2, \ldots, 500\}$ and various lag windows. Generally, if $Y_1, Y_2, \ldots, Y_N$ is a realization of a real-valued third-order stationary process $\{Y_t\}$ with mean v, autocovariance $C_2(s)$, and third cumulant $C_3(s_1, s_2)$, the smoothed spectrum, smoothed bispectrum, and smoothed normalized bispectrum are, respectively, given by (see [23])

$$\hat{f}(w) = \frac{1}{2\pi} \sum_{s=-(N-1)}^{N-1} \psi(s)\hat{C}_2(s)\exp(-isw)$$

$$= \frac{1}{2\pi} \sum_{s=-(N-1)}^{N-1} \psi(s)\hat{C}_2(s)cosws, \tag{9}$$

$$\hat{f}(w_1, w_2) = \frac{1}{4\pi^2} \sum_{s_1=-(N-1)}^{N-1} \sum_{s_2=-(N-1)}^{N-1} \psi(s_1, s_2)\hat{C}_3(s_1, s_2)\exp(-is_1 w_1 - is_2 w_2), \tag{10}$$

$$\hat{g}(w_1, w_2) = \frac{\hat{f}(w_1, w_2)}{\sqrt{\hat{f}(w_1)\hat{f}(w_2)\hat{f}(w_1 + w_2)}}, \tag{11}$$

where $\hat{C}_2(s)$ and $\hat{C}_3(s_1, s_2)$, the natural estimators for $C_2(s)$ and $C_3(s_1, s_2)$, are, respectively, given by

$$\hat{C}_2(s) = \frac{1}{N-s} \sum_{t=1}^{N-|s|} (Y_t - \bar{Y})(Y_{t+|s|} - \bar{Y}), \tag{12}$$

$$\bar{Y} = \frac{1}{N} \sum_{t=1}^{N} Y_t,$$

$$\hat{C}_3(s_1, s_2) = \frac{1}{N} \sum_{t=1}^{N-\alpha} (Y_t - \bar{Y})(Y_{t+s_1} - \bar{Y})(Y_{t+s_2} - \bar{Y}) \tag{13}$$

where $s_1, s_2 \geq 0, \alpha = max(0, s_1, s_2), s = 0, \pm 1, \pm 2, \ldots, \pm(N-1), -\pi \leq w_1, w_2 \leq \pi$, "$\psi(s)$" is a one-dimensional lag window and "$\psi(s_1, s_2)$" $= \psi(s_1 - s_2)\psi(s_1)\psi(s_2)$ is a two-dimensional lag window given by [32].

In this section, estimates of the spectral density functions are computed using the smoothed periodogram method based on the Daniell [33], Tukey [34], and Parzen lag windows [35] at a number of frequencies M = 8. This procedure is carried out for two cases, (i) the actual realizations or generated realizations from MCGINAR(1) shown in Figure 1 and (i) the anticipated realizations of the actual realizations based on FTSMC, shown in Figure 2.

Figures 6–8 show the estimates of the spectral density for the two scenarios: (i) the actual realizations from MCGINAR(1) and (ii) the anticipated realizations for MCGINAR(1) resulting from FTSMC, employing the Daniell, Parzen, and Tukey lag windows, respectively. Figures 9–11 show estimates of the bispectrum modulus for the two different scenarios: (i) actual realizations from MCGINAR(1) and (ii) anticipated realizations for MCGINAR(1) resulting from FTSMC, employing the Daniell, Parzen, and Tukey lag windows, respectively. Figures 12–14 show estimates of the normalized bispectrum modulus for two different scenarios: (i) actual realizations from MCGINAR(1) and (ii) anticipated real-

izations for MCGINAR(1) resulting from FTSMC, employing the Daniell, Parzen, and Tukey lag windows, respectively.

Extrapolation of Results

- The Tukey lag window with anticipated realizations is the best window in estimating $f_{YY}(w)$ compared to other windows, according to Figures 6–8 and the MSE that appears on each figure (for the calculation of the MSE, see [26,27]).
- The Daniell window with anticipated realizations is the best window in estimating $f_{YYY}(w_1, w_2)$ among the other lag windows, according to the MSE that appears in Figures 9–11, which is calculated from Tables 3–8.
- The Parzen window with anticipated realizations is the best window in estimating $g_{YYY}(w_1, w_2)$ among the other lag windows, according to the MSE that appears in Figures 12–14.
- These three points demonstrate the improvement in the smoothed estimates of the spectral density functions by the different windows in favor of anticipated realizations using FTSMC, as opposed to the realizations generated directly from the first-order MCGINAR process. This implies that FTSMC makes a positive contribution to smoothing estimation.
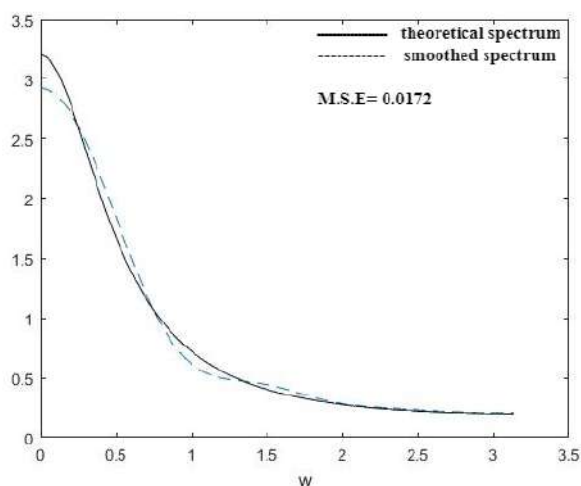
(**a**) actual realizations
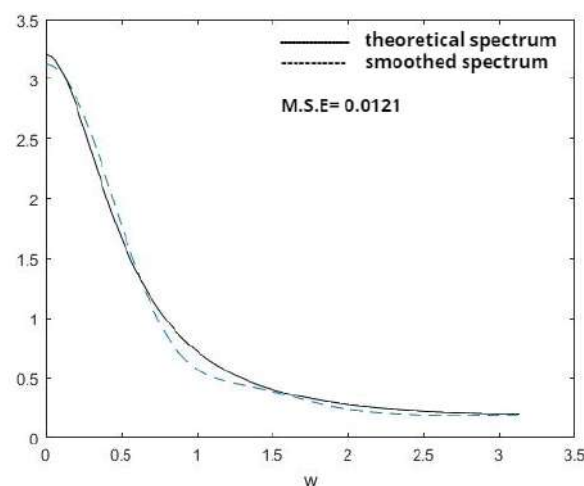
(**b**) anticipated realizations

Figure 6. Estimated spectrum with Daniell window.
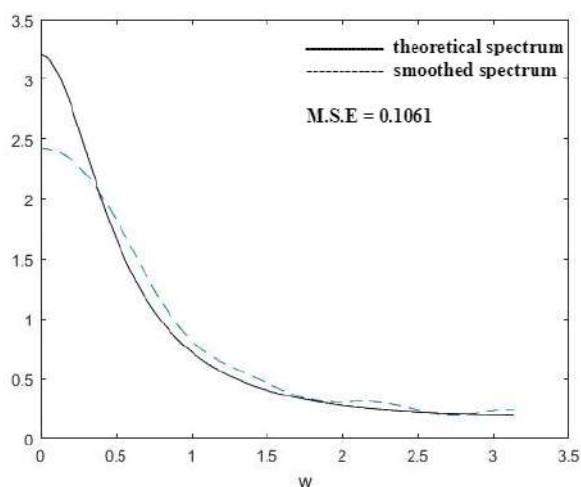
(**a**) actual realizations
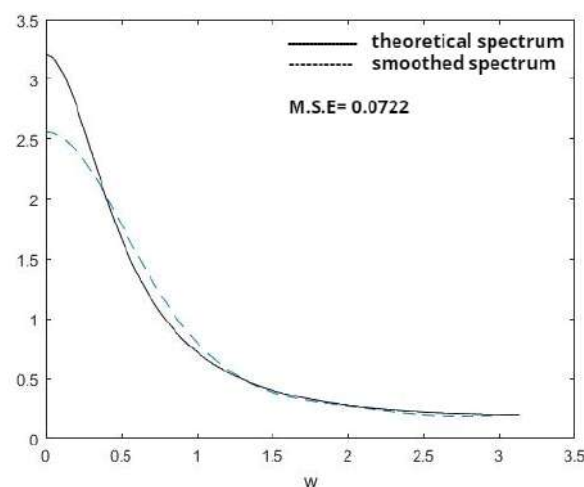
(**b**) anticipated realizations

Figure 7. Estimated spectrum with Parzen window.
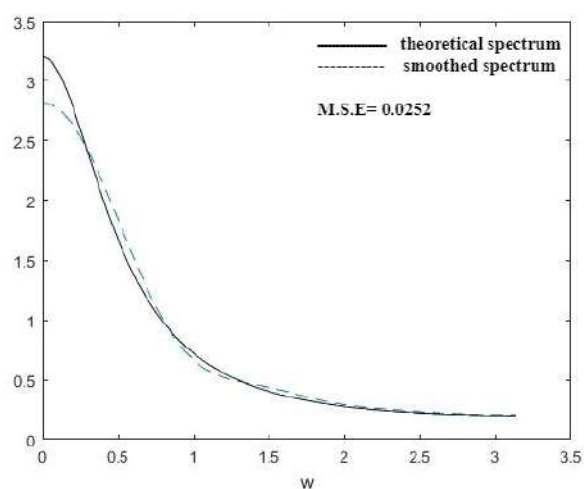
(**a**) actual realizations
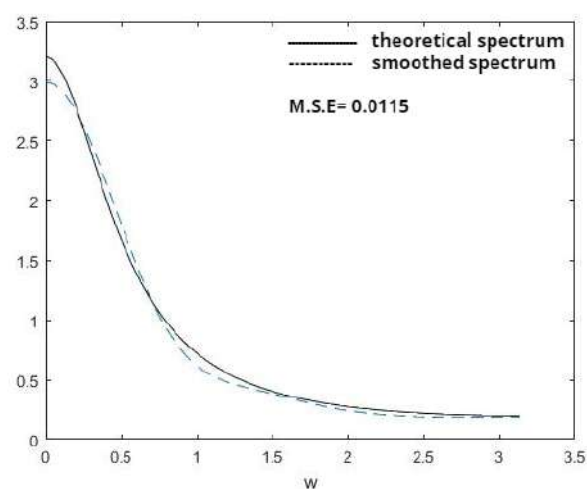
(**b**) anticipated realizations

Figure 8. Estimated spectrum with Tukey window.
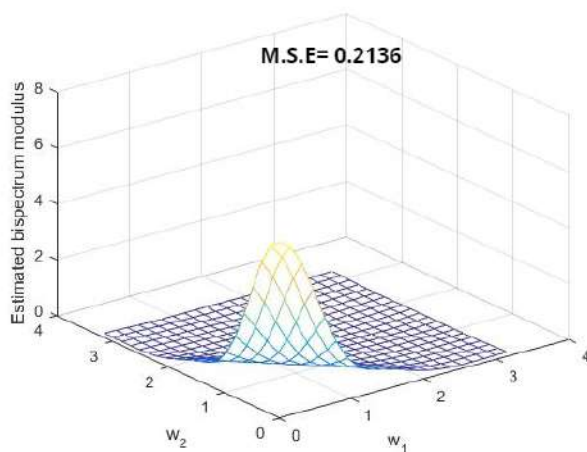
(**a**) actual realizations
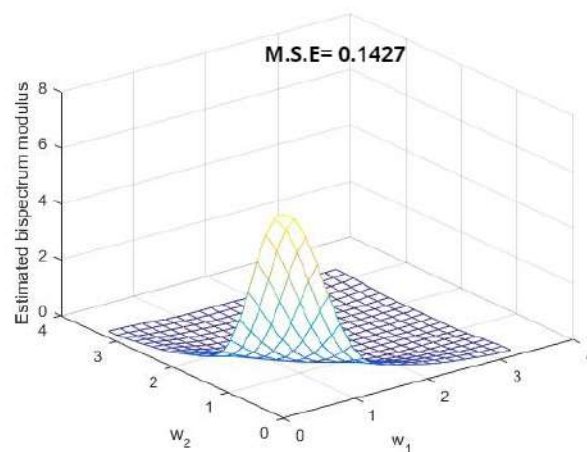
(**b**) anticipated realizations

Figure 9. Estimated bispectrum with Daniell window.
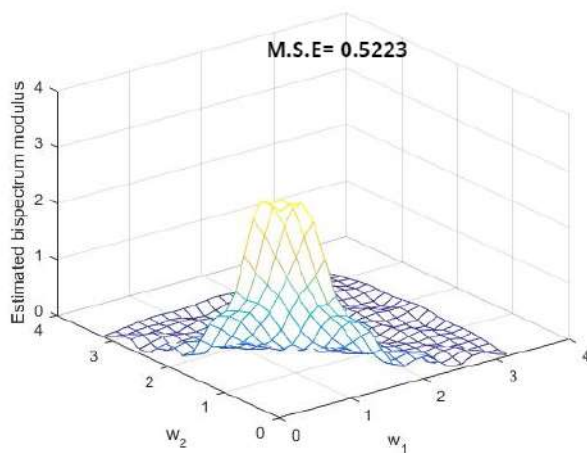
(**a**) actual realizations
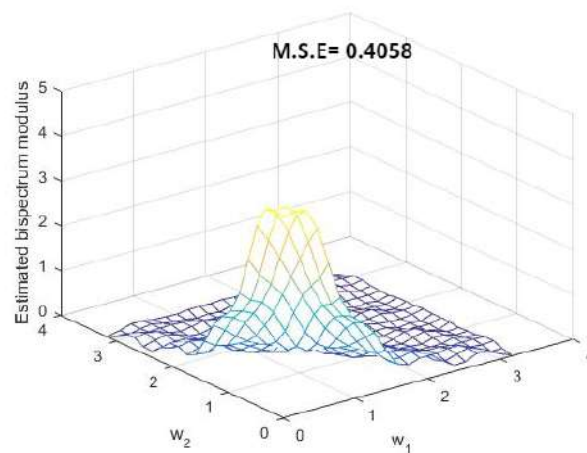
(**b**) anticipated realizations

Figure 10. Estimated bispectrum with Parzen window.
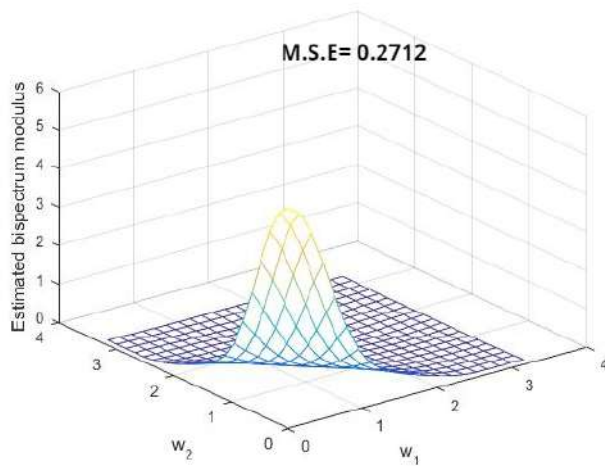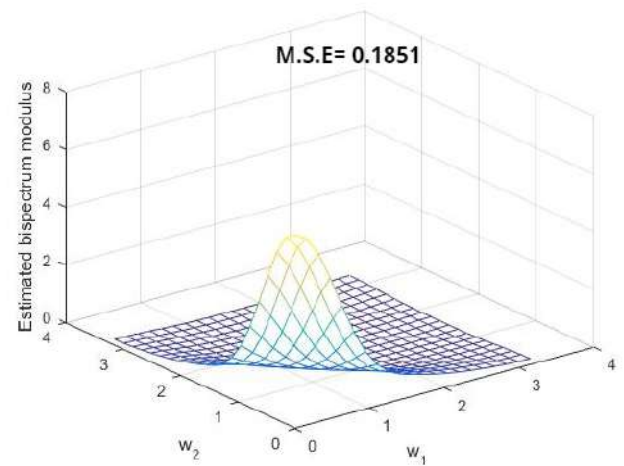
(**a**) actual realizations   (**b**) anticipated realizations

Figure 11. Estimated bispectrum with Tukey window.
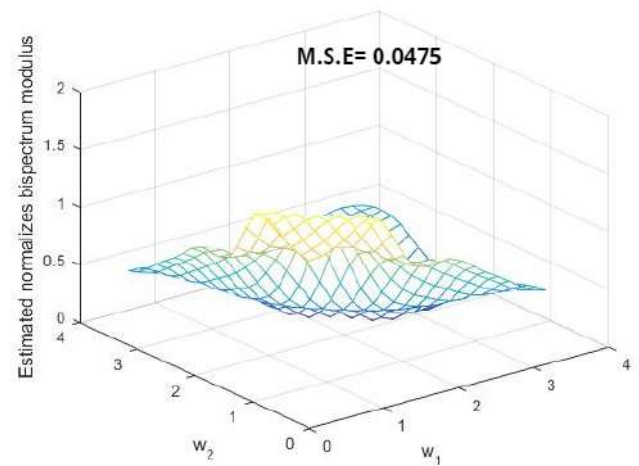
(**a**) actual realizations   (**b**) anticipated realizations

Figure 12. Estimated normalized bispectrum with Daniell window.
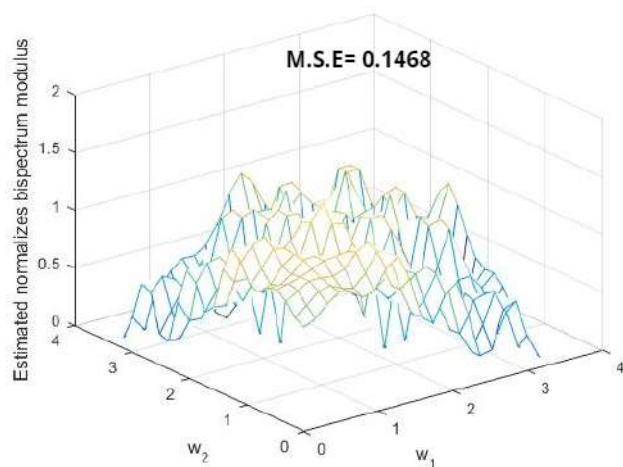
(**a**) actual realizations   (**b**) anticipated realizations

Figure 13. Estimated normalized bispectrum with Parzen window.

(**a**) actual realizations   (**b**) anticipated realizations

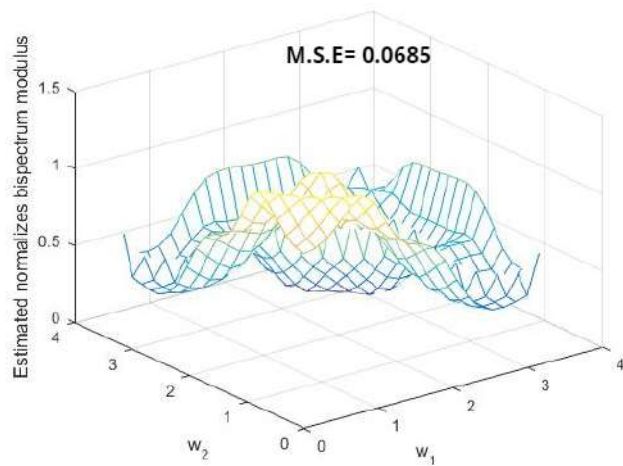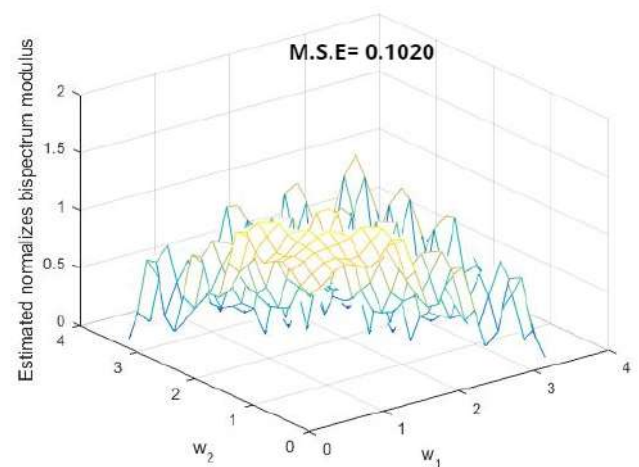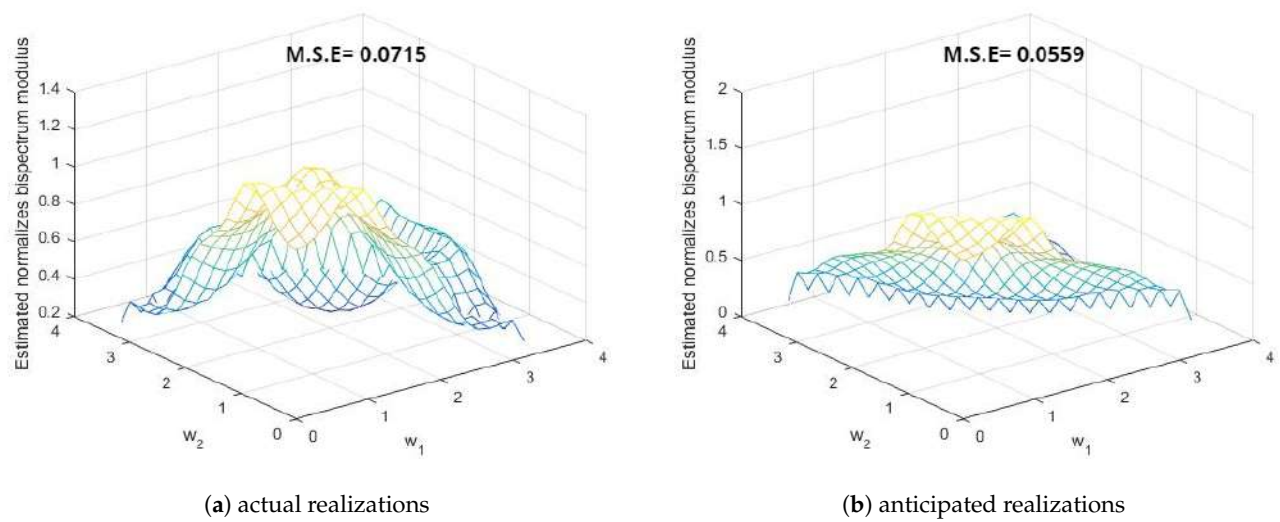**Figure 14.** Estimated normalized bispectrum with Tukey window.

Table 3. Numerical values of estimated bispectrum modulus of MCGINAR(1) using Daniell window with generated realizations.

w_2	0.00 π	0.05 π	0.10 π	0.15 π	0.20 π	0.25 π	0.30 π	0.35 π	0.40 π	0.45 π	0.50 π	0.55 π	0.60 π	0.65 π	0.70 π	0.75 π	0.80 π	0.85 π	0.90 π	0.95 π	π
w_1																					
0.00 π	6.2811	6.0178	5.2894	4.2634	3.1625	2.1953	1.4909	1.0680	0.8533	0.7378	0.6361	0.5164	0.3906	0.2837	0.2098	0.1671	0.1472	0.1429	0.1488	0.1578	0.1619
0.05 π	6.0178	5.5224	4.6485	3.5937	2.5750	1.7602	1.2203	0.9237	0.7751	0.6751	0.5663	0.4425	0.3258	0.2369	0.1810	0.1515	0.1400	0.1409	0.1485	0.1554	0.1554
0.10 π	5.2894	4.6485	3.7528	2.7993	1.9649	1.3559	0.9858	0.7926	0.6836	0.5860	0.4733	0.3572	0.2598	0.1930	0.1548	0.1364	0.1306	0.1334	0.1397	0.1429	0.1397
0.15 π	4.2634	3.5937	2.7993	2.0420	1.4374	1.0304	0.7970	0.6697	0.5776	0.4800	0.3742	0.2774	0.2048	0.1598	0.1362	0.1248	0.1213	0.1236	0.1273	0.1273	0.1236
0.20 π	3.1625	2.5750	1.9649	1.4374	1.0468	0.7963	0.6494	0.5536	0.4674	0.3768	0.2894	0.2179	0.1692	0.1413	0.1259	0.1170	0.1139	0.1152	0.1165	0.1152	0.1139
0.25 π	2.1953	1.7602	1.3559	1.0304	0.7963	0.6401	0.5339	0.4492	0.3702	0.2958	0.2320	0.1838	0.1524	0.1327	0.1188	0.1100	0.1073	0.1080	0.1080	0.1073	0.1100
0.30 π	1.4909	1.2203	0.9858	0.7970	0.6494	0.5339	0.4408	0.3634	0.2984	0.2444	0.2011	0.1683	0.1437	0.1239	0.1088	0.1006	0.0985	0.0986	0.0985	0.1006	0.1088
0.35 π	1.0680	0.9237	0.7926	0.6697	0.5536	0.4492	0.3634	0.2989	0.2518	0.2155	0.1848	0.1568	0.1309	0.1091	0.0940	0.0868	0.0851	0.0851	0.0868	0.0940	0.1091
0.40 π	0.8533	0.7751	0.6836	0.5776	0.4674	0.3702	0.2984	0.2518	0.2212	0.1955	0.1679	0.1383	0.1108	0.0895	0.0758	0.0695	0.0680	0.0695	0.0758	0.0895	0.1108
0.45 π	0.7378	0.6751	0.5860	0.4800	0.3768	0.2958	0.2444	0.2155	0.1955	0.1724	0.1431	0.1131	0.0883	0.0698	0.0573	0.0513	0.0513	0.0573	0.0698	0.0883	0.1131
0.50 π	0.6361	0.5663	0.4733	0.3742	0.2894	0.2320	0.2011	0.1848	0.1679	0.1431	0.1142	0.0890	0.0695	0.0535	0.0415	0.0370	0.0415	0.0535	0.0695	0.0890	0.1142
0.55 π	0.5164	0.4425	0.3572	0.2774	0.2179	0.1838	0.1683	0.1568	0.1383	0.1131	0.0890	0.0705	0.0550	0.0407	0.0313	0.0313	0.0407	0.0550	0.0705	0.0890	0.1131
0.60 π	0.3906	0.3258	0.2598	0.2048	0.1692	0.1524	0.1437	0.1309	0.1108	0.0883	0.0695	0.0550	0.0420	0.0316	0.0276	0.0316	0.0420	0.0550	0.0695	0.0883	0.1108
0.65 π	0.2837	0.2369	0.1930	0.1598	0.1413	0.1327	0.1239	0.1091	0.0895	0.0698	0.0535	0.0407	0.0316	0.0272	0.0272	0.0316	0.0407	0.0535	0.0698	0.0895	0.1091
0.70 π	0.2098	0.1810	0.1548	0.1362	0.1259	0.1188	0.1088	0.0940	0.0758	0.0573	0.0415	0.0313	0.0276	0.0272	0.0276	0.0313	0.0415	0.0573	0.0758	0.0940	0.1088
0.75 π	0.1671	0.1515	0.1364	0.1248	0.1170	0.1100	0.1006	0.0868	0.0695	0.0513	0.0370	0.0313	0.0316	0.0316	0.0313	0.0370	0.0513	0.0695	0.0868	0.1006	0.1100
0.80 π	0.1472	0.1400	0.1306	0.1213	0.1139	0.1073	0.0985	0.0851	0.0680	0.0513	0.0415	0.0407	0.0420	0.0407	0.0415	0.0513	0.0680	0.0851	0.0985	0.1073	0.1139
0.85 π	0.1429	0.1409	0.1334	0.1236	0.1152	0.1080	0.0986	0.0851	0.0695	0.0573	0.0535	0.0550	0.0550	0.0535	0.0573	0.0695	0.0851	0.0986	0.1080	0.1152	0.1236
0.90 π	0.1488	0.1485	0.1397	0.1273	0.1165	0.1080	0.0985	0.0868	0.0758	0.0698	0.0695	0.0705	0.0695	0.0698	0.0758	0.0868	0.0985	0.1080	0.1165	0.1273	0.1397
0.95 π	0.1578	0.1554	0.1429	0.1273	0.1152	0.1073	0.1006	0.0940	0.0895	0.0883	0.0890	0.0890	0.0883	0.0895	0.0940	0.1006	0.1073	0.1152	0.1273	0.1429	0.1554
π	0.1619	0.1554	0.1397	0.1236	0.1139	0.1100	0.1088	0.1091	0.1108	0.1131	0.1142	0.1131	0.1108	0.1091	0.1088	0.1100	0.1139	0.1236	0.1397	0.1554	0.1619

Table 4. Numerical values of estimated bispectrum modulus of MCGINAR(1) using Daniell window with anticipated realizations.

w_1 \ w_2	0.00 π	0.05 π	0.10 π	0.15 π	0.20 π	0.25 π	0.30 π	0.35 π	0.40 π	0.45 π	0.50 π	0.55 π	0.60 π	0.65 π	0.70 π	0.75 π	0.80 π	0.85 π	0.90 π	0.95 π	π
0.00 π	7.2751	7.0052	6.2479	5.1510	3.9273	2.7976	1.9240	1.3622	1.0610	0.9118	0.8128	0.7120	0.6067	0.5145	0.4451	0.3931	0.3476	0.3041	0.2662	0.2405	0.2315
0.05 π	7.0052	6.4921	5.5681	4.4160	3.2535	2.2711	1.5751	1.1641	0.9544	0.8384	0.7401	0.6355	0.5357	0.4560	0.3978	0.3517	0.3092	0.2702	0.2402	0.2240	0.2240
0.10 π	6.2479	5.5681	4.5956	3.5226	2.5369	1.7703	1.2666	0.9835	0.8314	0.7258	0.6231	0.5210	0.4338	0.3692	0.3221	0.2834	0.2489	0.2208	0.2031	0.1972	0.2031
0.15 π	5.1510	4.4160	3.5226	2.6376	1.8908	1.3491	1.0090	0.8133	0.6890	0.5839	0.4818	0.3907	0.3206	0.2717	0.2364	0.2084	0.1866	0.1730	0.1673	0.1673	0.1730
0.20 π	3.9273	3.2535	2.5369	1.8908	1.3815	1.0261	0.7997	0.6528	0.5394	0.4360	0.3431	0.2694	0.2182	0.1847	0.1622	0.1472	0.1396	0.1382	0.1386	0.1382	0.1396
0.25 π	2.7976	2.2711	1.7703	1.3491	1.0261	0.7951	0.6324	0.5080	0.4007	0.3058	0.2296	0.1764	0.1435	0.1242	0.1133	0.1091	0.1107	0.1139	0.1139	0.1107	0.1091
0.30 π	1.9240	1.5751	1.2666	1.0090	0.7997	0.6324	0.4973	0.3834	0.2856	0.2073	0.1526	0.1199	0.1021	0.0922	0.0869	0.0864	0.0892	0.0910	0.0892	0.0864	0.0869
0.35 π	1.3622	1.1641	0.9835	0.8133	0.6528	0.5080	0.3834	0.2799	0.1990	0.1433	0.1109	0.0942	0.0842	0.0757	0.0688	0.0663	0.0672	0.0672	0.0663	0.0688	0.0757
0.40 π	1.0610	0.9544	0.8314	0.6890	0.5394	0.4007	0.2856	0.1990	0.1413	0.1092	0.0942	0.0854	0.0750	0.0616	0.0506	0.0481	0.0491	0.0481	0.0506	0.0616	0.0750
0.45 π	0.9118	0.8384	0.7258	0.5839	0.4360	0.3058	0.2073	0.1433	0.1092	0.0952	0.0890	0.0802	0.0644	0.0456	0.0371	0.0409	0.0409	0.0371	0.0456	0.0644	0.0802
0.50 π	0.8128	0.7401	0.6231	0.4818	0.3431	0.2296	0.1526	0.1109	0.0942	0.0890	0.0833	0.0698	0.0491	0.0338	0.0384	0.0441	0.0384	0.0338	0.0491	0.0698	0.0833
0.55 π	0.7120	0.6355	0.5210	0.3907	0.2694	0.1764	0.1199	0.0942	0.0854	0.0802	0.0698	0.0520	0.0354	0.0378	0.0482	0.0482	0.0378	0.0354	0.0520	0.0698	0.0802
0.60 π	0.6067	0.5357	0.4338	0.3206	0.2182	0.1435	0.1021	0.0842	0.0750	0.0644	0.0491	0.0354	0.0381	0.0505	0.0564	0.0505	0.0381	0.0354	0.0491	0.0644	0.0750
0.65 π	0.5145	0.4560	0.3692	0.2717	0.1847	0.1242	0.0922	0.0757	0.0616	0.0456	0.0338	0.0378	0.0505	0.0595	0.0595	0.0505	0.0378	0.0338	0.0456	0.0616	0.0757
0.70 π	0.4451	0.3978	0.3221	0.2364	0.1622	0.1133	0.0869	0.0688	0.0506	0.0371	0.0384	0.0482	0.0564	0.0595	0.0564	0.0482	0.0384	0.0371	0.0506	0.0688	0.0869
0.75 π	0.3931	0.3517	0.2834	0.2084	0.1472	0.1091	0.0864	0.0663	0.0481	0.0409	0.0441	0.0482	0.0505	0.0505	0.0482	0.0441	0.0409	0.0481	0.0663	0.0864	0.1091
0.80 π	0.3476	0.3092	0.2489	0.1866	0.1396	0.1107	0.0892	0.0672	0.0491	0.0409	0.0384	0.0378	0.0381	0.0378	0.0384	0.0409	0.0491	0.0672	0.0892	0.1107	0.1396
0.85 π	0.3041	0.2702	0.2208	0.1730	0.1382	0.1139	0.0910	0.0672	0.0481	0.0371	0.0338	0.0354	0.0354	0.0338	0.0371	0.0481	0.0672	0.0910	0.1139	0.1382	0.1730
0.90 π	0.2662	0.2402	0.2031	0.1673	0.1386	0.1139	0.0892	0.0663	0.0506	0.0456	0.0491	0.0520	0.0491	0.0456	0.0506	0.0663	0.0892	0.1139	0.1386	0.1673	0.2031
0.95 π	0.2405	0.2240	0.1972	0.1673	0.1382	0.1107	0.0864	0.0688	0.0616	0.0644	0.0698	0.0698	0.0644	0.0616	0.0688	0.0864	0.1107	0.1382	0.1673	0.1972	0.2240
π	0.2315	0.2240	0.2031	0.1730	0.1396	0.1091	0.0869	0.0757	0.0750	0.0802	0.0833	0.0802	0.0750	0.0757	0.0869	0.1091	0.1396	0.1730	0.2031	0.2240	0.2315

Table 5. Numerical values of estimated bispectrum modulus of MCGINAR(1) using Parzen window with generated realizations.

w_2	0.00 π	0.05 π	0.10 π	0.15 π	0.20 π	0.25 π	0.30 π	0.35 π	0.40 π	0.45 π	0.50 π	0.55 π	0.60 π	0.65 π	0.70 π	0.75 π	0.80 π	0.85 π	0.90 π	0.95 π	π
w_1																					
0.00 π	3.6955	3.7475	3.7242	3.3375	2.6065	1.8893	1.4845	1.3180	1.1031	0.7373	0.4115	0.3208	0.3922	0.3916	0.2369	0.0834	0.0843	0.1780	0.1923	0.0956	0.0313
0.05 π	3.7475	3.7654	3.5645	2.9891	2.2462	1.6882	1.4204	1.2543	0.9559	0.5814	0.3719	0.3761	0.4317	0.3387	0.1525	0.0794	0.1357	0.2097	0.1510	0.0516	0.0516
0.10 π	3.7242	3.5645	3.1669	2.5556	1.9788	1.5756	1.3348	1.1040	0.7684	0.5145	0.4189	0.4249	0.3992	0.2327	0.1363	0.1160	0.1788	0.1871	0.0800	0.0815	0.0800
0.15 π	3.3375	2.9891	2.5556	2.1222	1.7260	1.3544	1.0771	0.8184	0.6098	0.5142	0.4139	0.3664	0.2636	0.1729	0.1725	0.1298	0.1721	0.1072	0.0982	0.0982	0.1072
0.20 π	2.6065	2.2462	1.9788	1.7260	1.3691	0.9940	0.7356	0.5862	0.5430	0.4511	0.3238	0.2446	0.1707	0.1929	0.1548	0.1376	0.1322	0.0839	0.1219	0.0839	0.1322
0.25 π	1.8893	1.6882	1.5756	1.3544	0.9940	0.6762	0.5309	0.5237	0.4931	0.3594	0.2361	0.1781	0.1993	0.2065	0.1530	0.1359	0.1113	0.1366	0.1366	0.1113	0.1359
0.30 π	1.4845	1.4204	1.3348	1.0771	0.7356	0.5309	0.5256	0.5543	0.4565	0.2778	0.1782	0.2132	0.2643	0.2140	0.1232	0.0946	0.1440	0.1911	0.1440	0.0946	0.1232
0.35 π	1.3180	1.2543	1.1040	0.8184	0.5862	0.5237	0.5543	0.5130	0.3328	0.1789	0.1825	0.2590	0.2524	0.1258	0.0272	0.0712	0.1733	0.1733	0.0712	0.0272	0.1258
0.40 π	1.1031	0.9559	0.7684	0.6098	0.5430	0.4931	0.4565	0.3328	0.1904	0.1739	0.1962	0.2302	0.1434	0.0117	0.0322	0.0879	0.1585	0.0879	0.0322	0.0117	0.1434
0.45 π	0.7373	0.5814	0.5145	0.5142	0.4511	0.3594	0.2778	0.1789	0.1739	0.1674	0.1873	0.1698	0.0543	0.0335	0.0350	0.1331	0.1331	0.0350	0.0335	0.0543	0.1698
0.50 π	0.4115	0.3719	0.4189	0.4139	0.3238	0.2361	0.1782	0.1825	0.1962	0.1873	0.1853	0.1293	0.0759	0.0785	0.1180	0.1572	0.1180	0.0785	0.0759	0.1293	0.1853
0.55 π	0.3208	0.3761	0.4249	0.3664	0.2446	0.1781	0.2132	0.2590	0.2302	0.1698	0.1293	0.1280	0.1517	0.1268	0.1123	0.1123	0.1268	0.1517	0.1280	0.1293	0.1698
0.60 π	0.3922	0.4317	0.3992	0.2636	0.1707	0.1993	0.2643	0.2524	0.1434	0.0543	0.0759	0.1517	0.1432	0.0530	0.0398	0.0530	0.1432	0.1517	0.0759	0.0543	0.1434
0.65 π	0.3916	0.3387	0.2327	0.1729	0.1929	0.2065	0.2140	0.1258	0.0117	0.0335	0.0785	0.1268	0.0530	0.0655	0.0655	0.0530	0.1268	0.0785	0.0335	0.0117	0.1258
0.70 π	0.2369	0.1525	0.1363	0.1725	0.1548	0.1530	0.1232	0.0272	0.0322	0.0350	0.1180	0.1123	0.0398	0.0655	0.0398	0.1123	0.1180	0.0350	0.0322	0.0272	0.1232
0.75 π	0.0834	0.0794	0.1160	0.1298	0.1376	0.1359	0.0946	0.0712	0.0879	0.1331	0.1572	0.1123	0.0530	0.0530	0.1123	0.1572	0.1331	0.0879	0.0712	0.0946	0.1359
0.80 π	0.0843	0.1357	0.1788	0.1721	0.1322	0.1113	0.1440	0.1733	0.1585	0.1331	0.1180	0.1268	0.1432	0.1268	0.1180	0.1331	0.1585	0.1733	0.1440	0.1113	0.1322
0.85 π	0.1780	0.2097	0.1871	0.1072	0.0839	0.1366	0.1911	0.1733	0.0879	0.0350	0.0785	0.1517	0.1517	0.0785	0.0350	0.0879	0.1733	0.1911	0.1366	0.0839	0.1072
0.90 π	0.1923	0.1510	0.0800	0.0982	0.1219	0.1366	0.1440	0.0712	0.0322	0.0335	0.0759	0.1280	0.0759	0.0335	0.0322	0.0712	0.1440	0.1366	0.1219	0.0982	0.0800
0.95 π	0.0956	0.0516	0.0815	0.0982	0.0839	0.1113	0.0946	0.0272	0.0117	0.0543	0.1293	0.1293	0.0543	0.0117	0.0272	0.0946	0.1113	0.0839	0.0982	0.0815	0.0516
π	0.0313	0.0516	0.0800	0.1072	0.1322	0.1359	0.1232	0.1258	0.1434	0.1698	0.1853	0.1698	0.1434	0.1258	0.1232	0.1359	0.1322	0.1072	0.0800	0.0516	0.0313

Table 6. Numerical values of estimated bispectrum modulus of MCGINAR(1) using Parzen window with anticipated realizations.

w_2	0.00 π	0.05 π	0.10 π	0.15 π	0.20 π	0.25 π	0.30 π	0.35 π	0.40 π	0.45 π	0.50 π	0.55 π	0.60 π	0.65 π	0.70 π	0.75 π	0.80 π	0.85 π	0.90 π	0.95 π	π
w_1																					
0.00 π	4.4795	4.5332	4.4906	4.0266	3.1702	2.3340	1.8538	1.6362	1.3547	0.9068	0.5249	0.4285	0.5160	0.5075	0.3180	0.1420	0.1554	0.2679	0.2661	0.1242	0.0350
0.05 π	4.5332	4.5419	4.2940	3.6252	2.7681	2.1131	1.7767	1.5430	1.1704	0.7348	0.4954	0.5049	0.5632	0.4509	0.2407	0.1582	0.2317	0.3022	0.2169	0.0872	0.0872
0.10 π	4.4906	4.2940	3.8391	3.1574	2.4899	1.9927	1.6605	1.3497	0.9690	0.6803	0.5593	0.5588	0.5226	0.3567	0.2459	0.2259	0.2758	0.2677	0.1656	0.1444	0.1656
0.15 π	4.0266	3.6252	3.1574	2.6758	2.1861	1.7004	1.3202	1.0149	0.7901	0.6529	0.5189	0.4498	0.3566	0.2918	0.2740	0.2123	0.2148	0.1684	0.1806	0.1806	0.1684
0.20 π	3.1702	2.7681	2.4899	2.1861	1.7145	1.2121	0.8855	0.7296	0.6677	0.5248	0.3472	0.2608	0.2308	0.2768	0.2083	0.1323	0.1236	0.1282	0.1894	0.1282	0.1236
0.25 π	2.3340	2.1131	1.9927	1.7004	1.2121	0.7995	0.6362	0.6340	0.5721	0.3697	0.2137	0.1702	0.2385	0.2451	0.1347	0.1160	0.0962	0.1689	0.1689	0.0962	0.1160
0.30 π	1.8538	1.7767	1.6605	1.3202	0.8855	0.6362	0.6323	0.6537	0.5055	0.2720	0.1623	0.2237	0.2984	0.2236	0.1021	0.0801	0.1538	0.2244	0.1538	0.0801	0.1021
0.35 π	1.6362	1.5430	1.3497	1.0149	0.7296	0.6340	0.6537	0.5863	0.3705	0.1906	0.1920	0.2820	0.2756	0.1364	0.0346	0.0849	0.1958	0.1958	0.0849	0.0346	0.1364
0.40 π	1.3547	1.1704	0.9690	0.7901	0.6677	0.5721	0.5055	0.3705	0.2263	0.1897	0.1948	0.2214	0.1420	0.0638	0.0713	0.0866	0.1444	0.0866	0.0713	0.0638	0.1420
0.45 π	0.9068	0.7348	0.6803	0.6529	0.5248	0.3697	0.2720	0.1906	0.1897	0.1505	0.1452	0.1350	0.0385	0.0732	0.0260	0.1047	0.1047	0.0260	0.0732	0.0385	0.1350
0.50 π	0.5249	0.4954	0.5593	0.5189	0.3472	0.2137	0.1623	0.1920	0.1948	0.1452	0.1573	0.1027	0.0760	0.0775	0.0976	0.1549	0.0976	0.0775	0.0760	0.1027	0.1573
0.55 π	0.4285	0.5049	0.5588	0.4498	0.2608	0.1702	0.2237	0.2820	0.2214	0.1350	0.1027	0.1178	0.1672	0.1200	0.1079	0.1079	0.1200	0.1672	0.1178	0.1027	0.1350
0.60 π	0.5160	0.5632	0.5226	0.3566	0.2308	0.2385	0.2984	0.2756	0.1420	0.0385	0.0760	0.1672	0.1616	0.0546	0.0297	0.0546	0.1616	0.1672	0.0760	0.0385	0.1420
0.65 π	0.5075	0.4509	0.3567	0.2918	0.2768	0.2451	0.2236	0.1364	0.0638	0.0732	0.0775	0.1200	0.0546	0.0492	0.0492	0.0546	0.1200	0.0775	0.0732	0.0638	0.1364
0.70 π	0.3180	0.2407	0.2459	0.2740	0.2083	0.1347	0.1021	0.0346	0.0713	0.0260	0.0976	0.1079	0.0297	0.0492	0.0297	0.1079	0.0976	0.0260	0.0713	0.0346	0.1021
0.75 π	0.1420	0.1582	0.2259	0.2123	0.1323	0.1160	0.0801	0.0849	0.0866	0.1047	0.1549	0.1079	0.0546	0.0546	0.1079	0.1549	0.1047	0.0866	0.0849	0.0801	0.1160
0.80 π	0.1554	0.2317	0.2758	0.2148	0.1236	0.0962	0.1538	0.1958	0.1444	0.1047	0.0976	0.1200	0.1616	0.1200	0.0976	0.1047	0.1444	0.1958	0.1538	0.0962	0.1236
0.85 π	0.2679	0.3022	0.2677	0.1684	0.1282	0.1689	0.2244	0.1958	0.0866	0.0260	0.0775	0.1672	0.1672	0.0775	0.0260	0.0866	0.1958	0.2244	0.1689	0.1282	0.1684
0.90 π	0.2661	0.2169	0.1656	0.1806	0.1894	0.1689	0.1538	0.0849	0.0713	0.0732	0.0760	0.1178	0.0760	0.0732	0.0713	0.0849	0.1538	0.1689	0.1894	0.1806	0.1656
0.95 π	0.1242	0.0872	0.1444	0.1806	0.1282	0.0962	0.0801	0.0346	0.0638	0.0385	0.1027	0.1027	0.0385	0.0638	0.0346	0.0801	0.0962	0.1282	0.1806	0.1444	0.0872
π	0.0350	0.0872	0.1656	0.1684	0.1236	0.1160	0.1021	0.1364	0.1420	0.1350	0.1573	0.1350	0.1420	0.1364	0.1021	0.1160	0.1236	0.1684	0.1656	0.0872	0.0350

Table 7. Numerical values of estimated bispectrum modulus of MCGINAR(1) using Tukey window with generated realizations.

w_2	0.00 π	0.05π	0.10 π	0.15π	0.20 π	0.25π	0.30 π	0.35π	0.40 π	0.45π	0.50 π	0.55π	0.60 π	0.65π	0.70 π	0.75π	0.80 π	0.85π	0.90 π	0.95π	π
w_1																					
0.00 π	5.7134	5.4997	4.9012	4.0391	3.0884	2.2251	1.5656	1.1330	0.8751	0.7145	0.5925	0.4825	0.3789	0.2852	0.2093	0.1591	0.1362	0.1323	0.1348	0.1362	0.1363
0.05 π	5.4997	5.0938	4.3649	3.4631	2.5661	1.8210	1.2955	0.9698	0.7746	0.6407	0.5279	0.4225	0.3249	0.2407	0.1782	0.1428	0.1309	0.1310	0.1327	0.1328	0.1328
0.10 π	4.9012	4.3649	3.5997	2.7630	2.0076	1.4310	1.0507	0.8198	0.6712	0.5558	0.4518	0.3549	0.2682	0.1983	0.1522	0.1307	0.1256	0.1256	0.1249	0.1242	0.1249
0.15 π	4.0391	3.4631	2.7630	2.0763	1.5091	1.1062	0.8493	0.6861	0.5674	0.4661	0.3734	0.2893	0.2178	0.1652	0.1349	0.1232	0.1201	0.1179	0.1156	0.1156	0.1179
0.20 π	3.0884	2.5661	2.0076	1.5091	1.1261	0.8636	0.6905	0.5677	0.4686	0.3815	0.3034	0.2352	0.1809	0.1445	0.1260	0.1187	0.1146	0.1106	0.1088	0.1106	0.1146
0.25 π	2.2251	1.8210	1.4310	1.1062	0.8636	0.6910	0.5648	0.4655	0.3827	0.3114	0.2494	0.1974	0.1581	0.1332	0.1203	0.1133	0.1078	0.1041	0.1041	0.1078	0.1133
0.30 π	1.5656	1.2955	1.0507	0.8493	0.6905	0.5648	0.4636	0.3817	0.3151	0.2595	0.2124	0.1733	0.1437	0.1240	0.1119	0.1038	0.0983	0.0962	0.0983	0.1038	0.1119
0.35 π	1.1330	0.9698	0.8198	0.6861	0.5677	0.4655	0.3817	0.3161	0.2648	0.2230	0.1868	0.1553	0.1298	0.1113	0.0985	0.0900	0.0857	0.0857	0.0900	0.0985	0.1113
0.40 π	0.8751	0.7746	0.6712	0.5674	0.4686	0.3827	0.3151	0.2648	0.2268	0.1949	0.1648	0.1365	0.1126	0.0944	0.0816	0.0739	0.0714	0.0739	0.0816	0.0944	0.1126
0.45 π	0.7145	0.6407	0.5558	0.4661	0.3815	0.3114	0.2595	0.2230	0.1949	0.1685	0.1411	0.1150	0.0931	0.0762	0.0642	0.0580	0.0580	0.0642	0.0762	0.0931	0.1150
0.50 π	0.5925	0.5279	0.4518	0.3734	0.3034	0.2494	0.2124	0.1868	0.1648	0.1411	0.1163	0.0934	0.0743	0.0591	0.0487	0.0449	0.0487	0.0591	0.0743	0.0934	0.1163
0.55 π	0.4825	0.4225	0.3549	0.2893	0.2352	0.1974	0.1733	0.1553	0.1365	0.1150	0.0934	0.0740	0.0575	0.0445	0.0370	0.0370	0.0445	0.0575	0.0740	0.0934	0.1150
0.60 π	0.3789	0.3249	0.2682	0.2178	0.1809	0.1581	0.1437	0.1298	0.1126	0.0931	0.0743	0.0575	0.0436	0.0341	0.0308	0.0341	0.0436	0.0575	0.0743	0.0931	0.1126
0.65 π	0.2852	0.2407	0.1983	0.1652	0.1445	0.1332	0.1240	0.1113	0.0944	0.0762	0.0591	0.0445	0.0341	0.0293	0.0293	0.0341	0.0445	0.0591	0.0762	0.0944	0.1113
0.70 π	0.2093	0.1782	0.1522	0.1349	0.1260	0.1203	0.1119	0.0985	0.0816	0.0642	0.0487	0.0370	0.0308	0.0293	0.0308	0.0370	0.0487	0.0642	0.0816	0.0985	0.1119
0.75 π	0.1591	0.1428	0.1307	0.1232	0.1187	0.1133	0.1038	0.0900	0.0739	0.0580	0.0449	0.0370	0.0341	0.0341	0.0370	0.0449	0.0580	0.0739	0.0900	0.1038	0.1133
0.80 π	0.1362	0.1309	0.1256	0.1201	0.1146	0.1078	0.0983	0.0857	0.0714	0.0580	0.0487	0.0445	0.0436	0.0445	0.0487	0.0580	0.0714	0.0857	0.0983	0.1078	0.1146
0.85 π	0.1323	0.1310	0.1256	0.1179	0.1106	0.1041	0.0962	0.0857	0.0739	0.0642	0.0591	0.0575	0.0575	0.0591	0.0642	0.0739	0.0857	0.0962	0.1041	0.1106	0.1179
0.90 π	0.1348	0.1327	0.1249	0.1156	0.1088	0.1041	0.0983	0.0900	0.0816	0.0762	0.0743	0.0740	0.0743	0.0762	0.0816	0.0900	0.0983	0.1041	0.1088	0.1156	0.1249
0.95 π	0.1362	0.1328	0.1242	0.1156	0.1106	0.1078	0.1038	0.0985	0.0944	0.0931	0.0934	0.0934	0.0931	0.0944	0.0985	0.1038	0.1078	0.1106	0.1156	0.1242	0.1328
π	0.1363	0.1328	0.1249	0.1179	0.1146	0.1133	0.1119	0.1113	0.1126	0.1150	0.1163	0.1150	0.1126	0.1113	0.1119	0.1133	0.1146	0.1179	0.1249	0.1328	0.1363

Table 8. Numerical values of estimated bispectrum modulus of MCGINAR(1) using Tukey window with anticipated realizations.

w_1 \ w_2	0.00 π	0.05π	0.10 π	0.15π	0.20 π	0.25π	0.30 π	0.35π	0.40 π	0.45π	0.50 π	0.55π	0.60 π	0.65π	0.70 π	0.75π	0.80 π	0.85π	0.90 π	0.95π	π
0.00 π	6.6935	6.4649	5.8204	4.8787	3.8135	2.8089	2.0016	1.4428	1.1004	0.8989	0.7664	0.6600	0.5655	0.4828	0.4138	0.3578	0.3118	0.2732	0.2414	0.2194	0.2114
0.05 π	6.4649	6.0287	5.2377	4.2400	3.2157	2.3250	1.6601	1.2270	0.9685	0.8093	0.6930	0.5934	0.5053	0.4304	0.3693	0.3201	0.2796	0.2459	0.2201	0.2056	0.2056
0.10 π	5.8204	5.2377	4.3955	3.4515	2.5641	1.8474	1.3433	1.0251	0.8299	0.6973	0.5913	0.4991	0.4200	0.3552	0.3041	0.2639	0.2317	0.2065	0.1895	0.1834	0.1895
0.15 π	4.8787	4.2400	3.4515	2.6532	1.9587	1.4305	1.0711	0.8406	0.6866	0.5704	0.4733	0.3908	0.3233	0.2711	0.2321	0.2031	0.1817	0.1665	0.1583	0.1583	0.1665
0.20 π	3.8135	3.2157	2.5641	1.9587	1.4634	1.0989	0.8483	0.6754	0.5464	0.4422	0.3556	0.2857	0.2325	0.1946	0.1687	0.1518	0.1408	0.1339	0.1313	0.1339	0.1408
0.25 π	2.8089	2.3250	1.8474	1.4305	1.0989	0.8517	0.6701	0.5309	0.4187	0.3270	0.2543	0.1999	0.1621	0.1381	0.1239	0.1161	0.1112	0.1083	0.1083	0.1112	0.1161
0.30 π	2.0016	1.6601	1.3433	1.0711	0.8483	0.6701	0.5261	0.4077	0.3110	0.2354	0.1798	0.1418	0.1179	0.1040	0.0962	0.0912	0.0873	0.0857	0.0873	0.0912	0.0962
0.35 π	1.4428	1.2270	1.0251	0.8406	0.6754	0.5309	0.4077	0.3063	0.2279	0.1715	0.1336	0.1094	0.0942	0.0839	0.0760	0.0695	0.0655	0.0655	0.0695	0.0760	0.0839
0.40 π	1.1004	0.9685	0.8299	0.6866	0.5464	0.4187	0.3110	0.2279	0.1696	0.1320	0.1084	0.0926	0.0799	0.0679	0.0577	0.0512	0.0492	0.0512	0.0577	0.0679	0.0799
0.45 π	0.8989	0.8093	0.6973	0.5704	0.4422	0.3270	0.2354	0.1715	0.1320	0.1089	0.0940	0.0809	0.0667	0.0527	0.0439	0.0419	0.0419	0.0439	0.0527	0.0667	0.0809
0.50 π	0.7664	0.6930	0.5913	0.4733	0.3556	0.2543	0.1798	0.1336	0.1084	0.0940	0.0821	0.0683	0.0528	0.0416	0.0403	0.0419	0.0403	0.0416	0.0528	0.0683	0.0821
0.55 π	0.6600	0.5934	0.4991	0.3908	0.2857	0.1999	0.1418	0.1094	0.0926	0.0809	0.0683	0.0536	0.0418	0.0403	0.0447	0.0447	0.0403	0.0418	0.0536	0.0683	0.0809
0.60 π	0.5655	0.5053	0.4200	0.3233	0.2325	0.1621	0.1179	0.0942	0.0799	0.0667	0.0528	0.0418	0.0404	0.0464	0.0498	0.0464	0.0404	0.0418	0.0528	0.0667	0.0799
0.65 π	0.4828	0.4304	0.3552	0.2711	0.1946	0.1381	0.1040	0.0839	0.0679	0.0527	0.0416	0.0403	0.0464	0.0519	0.0519	0.0464	0.0403	0.0416	0.0527	0.0679	0.0839
0.70 π	0.4138	0.3693	0.3041	0.2321	0.1687	0.1239	0.0962	0.0760	0.0577	0.0439	0.0403	0.0447	0.0498	0.0519	0.0498	0.0447	0.0403	0.0439	0.0577	0.0760	0.0962
0.75 π	0.3578	0.3201	0.2639	0.2031	0.1518	0.1161	0.0912	0.0695	0.0512	0.0419	0.0419	0.0447	0.0464	0.0464	0.0447	0.0419	0.0419	0.0512	0.0695	0.0912	0.1161
0.80 π	0.3118	0.2796	0.2317	0.1817	0.1408	0.1112	0.0873	0.0655	0.0492	0.0419	0.0403	0.0403	0.0404	0.0403	0.0403	0.0419	0.0492	0.0655	0.0873	0.1112	0.1408
0.85 π	0.2732	0.2459	0.2065	0.1665	0.1339	0.1083	0.0857	0.0655	0.0512	0.0439	0.0416	0.0418	0.0418	0.0416	0.0439	0.0512	0.0655	0.0857	0.1083	0.1339	0.1665
0.90 π	0.2414	0.2201	0.1895	0.1583	0.1313	0.1083	0.0873	0.0695	0.0577	0.0527	0.0528	0.0536	0.0528	0.0527	0.0577	0.0695	0.0873	0.1083	0.1313	0.1583	0.1895
0.95 π	0.2194	0.2056	0.1834	0.1583	0.1339	0.1112	0.0912	0.0760	0.0679	0.0667	0.0683	0.0683	0.0667	0.0679	0.0760	0.0912	0.1112	0.1339	0.1583	0.1834	0.2056
π	0.2114	0.2056	0.1895	0.1665	0.1408	0.1161	0.0962	0.0839	0.0799	0.0809	0.0821	0.0809	0.0799	0.0839	0.0962	0.1161	0.1408	0.1665	0.1895	0.2056	0.2114

6. Conclusions

A novel approach known as the FTSMC method has been suggested to derive more accurate smoothing estimates of spectral density functions. For this reason, the smoothed estimates of the spectral, bispectral, and normalized bispectral density functions for a known process (MCGINAR(1)) are computed. Both generated realizations from the specified model and anticipated realizations resulting from the FTSMC approach are used to calculate the estimates of these functions. The results and illustrations in this research demonstrate that the FTSMC enhances the estimate's smoothing. Future studies will try to enhance the mentioned method using long short-term memory and pi-sigma artificial neural networks to produce the best smoothing of estimates in comparison to the conclusions obtained here.

References

1. Song, Q.; Chissom, B.S. Fuzzy time series and its models. *Fuzzy Sets Syst.* **1993**, *54*, 269–277. [CrossRef]
2. Alyousifi, Y.; Othman, M.; Almohammedi, A.A. A novel stochastic fuzzy time series forecasting model based on a new partition method. *IEEE Access* **2021**, *9*, 80236–80252. [CrossRef]
3. Alyousifi, Y.; Othman, M.; Sokkalingam, R.; Faye, I.; Silva, P.C. Predicting daily air pollution index based on fuzzy time series markov chain model. *Symmetry* **2020**, *12*, 293. [CrossRef]
4. Hariyanto, S.; Udjiani, T. Fuzzy time series Markov Chain and Fuzzy time series Chen & Hsu for forecasting. *J. Phys. Conf. Ser.* **2021**, *1943*, 012128.
5. Salawudeen, A.T.; Mu'azu, M.B.; Adedokun, E.A.; Baba, B.A. Optimal determination of hidden Markov model parameters for fuzzy time series forecasting. *Sci. Afr.* **2022**, *16*, e01174. [CrossRef]
6. McKenzie, E. Autoregressive moving-average processes with negative-binomial and geometric marginal distributions. *Adv. Appl. Probab.* **1986**, *18*, 679–705. [CrossRef]
7. Al-Osh, M.A.; Aly, E.A.A. First order autoregressive time series with negative binomial and geometric marginals. *Commun. Stat.-Theory Methods* **1992**, *21*, 2483–2492. [CrossRef]
8. Alzaid, A.; Al-Osh, M. First-order integer-valued autoregressive (INAR(1)) process: Distributional and regression properties. *Stat. Neerl.* **1988**, *42*, 53–61. [CrossRef]
9. Bakouch, H.S.; Ristić, M.M. Zero truncated Poisson integer-valued AR(1) model. *Metrika* **2010**, *72*, 265–280. [CrossRef]
10. Alzaid, A.A.; Al-Osh, M.A. Some autoregressive moving average processes with generalized Poisson marginal distributions. *Ann. Inst. Stat. Math.* **1993**, *45*, 223–232. [CrossRef]
11. Jin-Guan, D.; Yuan, L. The integer-valued autoregressive (INAR(p)) model. *J. Time Ser. Anal.* **1991**, *12*, 129–142. [CrossRef]
12. Aly, E.A.A.; Bouzar, N. Explicit stationary distributions for some Galton-Watson processes with immigration. *Stoch. Models* **1994**, *10*, 499–517. [CrossRef]
13. Latour, A. Existence and stochastic structure of a non-negative integer-valued autoregressive process. *J. Time Ser. Anal.* **1998**, *19*, 439–455. [CrossRef]
14. Ristić, M.M.; Bakouch, H.S.; Nastić, A.S. A new geometric first-order integer-valued autoregressive (NGINAR(1)) process. *J. Stat. Plan. Inference* **2009**, *139*, 2218–2226. [CrossRef]

15. Ristić, M.M.; Nastić, A.S.; Bakouch, H.S. Estimation in an integer-valued autoregressive process with negative binomial marginals (NBINAR(1)). *Commun.-Stat. Theory Methods* **2012**, *41*, 606–618. [CrossRef]

16. Ristić, M.M.; Nastić, A.S.; Jayakumar, K.; Bakouch, H.S. A bivariate INAR(1) time series model with geometric marginals. *Appl. Math. Lett.* **2012**, *25*, 481–485. [CrossRef]

17. Nastić, A.S.; Ristić, M.M. Some geometric mixed integer-valued autoregressive (INAR) models. *Stat. Probab. Lett.* **2012**, *82*, 805–811. [CrossRef]

18. Nastić, A.S.; Ristić, M.M.; Bakouch, H.S. A combined geometric INAR(p) model based on negative binomial thinning. *Math. Comput. Model.* **2012**, *55*, 1665–1672. [CrossRef]

19. Zheng, H.; Basawa, I.V.; Datta, S. First-order random coefficient integer-valued autoregressive processes. *J. Stat. Plan. Inference* **2007**, *137*, 212–229. [CrossRef]

20. Gomes, D.; Castro, L.C. Generalized integer-valued random coefficient for a first order structure autoregressive (RCINAR) process. *J. Stat. Plan. Inference* **2009**, *139*, 4088–4097. [CrossRef]

21. Wang, D.; Zhang, H. Generalized RCINAR(p) process with signed thinning operator. *Commun. Stat. Comput.* **2010**, *40*, 13–44. [CrossRef]

22. Ristić, M.M.; Nastić, A.S.; Miletić, A.V. A geometric time series model with dependent Bernoulli counting series. *J. Time Ser. Anal.* **2013**, *34*, 466–476. [CrossRef]

23. Gabr, M.M.; El-Desouky, B.S.; Shiha, F.A.; El-Hadidy, S.M. Higher Order Moments, Spectral and Bispectral Density Functions for INAR(1). *Int. J. Comput. Appl.* **2018**, *182*, 0975–8887.

24. Miletić, A.V.; Ristić, M.M.; Nastić, A.S.; Bakouch, H.S. An INAR(1) model based on a mixed dependent and independent counting series. *J. Stat. Comput. Simul.* **2018**, *88*, 290–304. [CrossRef]

25. Teamah, A.A.M.; Faied, H.M.; El-Menshawy, M.H. Effect of Fuzzy Time Series Technique on Estimators of Spectral Analysis. In *Recent Advances in Mathematical Research and Computer Science*; B P International: London, UK, 2022; Volume 6, pp. 29–38.

26. El-menshawy, M.H.; Teamah, A.A.M.; Abu-Youssef, S.E.; Faied, H.M. Higher Order Moments, Cumulants, Spectral and Bispectral Density Functions of the ZTPINAR(1) Process. *Appl. Math* **2022**, *16*, 213–225.

27. El-Morshedy, M.; El-Menshawy, M.H.; Almazah, M.M.A.; El-Sagheer, R.M.; Eliwa, M.S. Effect of fuzzy time series on smoothing estimation of the INAR(1) process. *Axioms* **2022**, *11*, 423. [CrossRef]

28. Afnisah, N.; Marpaung, F. A Comparison of the Fuzzy Time Series Methods of Chen, Cheng and Markov Chain in Predicting Rainfall in Medan. *J. Phys. Conf. Ser.* **2020**, *1462*, 012044.

29. Rukhansah, N.; Muslim, M.A.; Arifudin, R. Peramalan Harga Emas Menggunakan Fuzzy Time Series Markov Chain Model. *Komputaki* **2016**, *2*.

30. Safitri, Y.; Wahyuningsih, S.; Goejantoro, R. Peramalan Dengan Metode Fuzzy Time Series Markov Chain. *Eksponensial* **2018**, *9*, 51–58.

31. Steutel, F.W.; van Harn, K. Discrete analogues of self-decomposability and stability. In *The Annals of Probability*; Institute of Mathematical Statistics: Beachwood, OH, USA, 1979; pp. 893–899.

32. Rao, T.S.; Gabr, M.M. *An Introduction to Bispectral Analysis and Bilinear Time Series Models*; Springer Science & Business Media: Berlin, Germany, 1984; Volume 24.

33. Daniell, P.J. Discussion on symposium on autocorrelation in time series. *J. R. Stat. Soc.* **1946**, *8*, 88–90.

34. Blackman, R.B.; Tukey, J.W. Particular pairs of windows. In *The Measurement of Power Spectra, from the Point of View of Communications Engineering*; Nokia Bell Labs: Murray Hill, NJ, USA, 1959; pp. 98–99.

35. Parzen, E. Mathematical considerations in the estimation of spectra. *Technometrics* **1961**, *3*, 167–190. [CrossRef]